Geomechanics and Engineering, *Vol. 30, No. 3 (2022) 293-312*
https://doi.org/10.12989/gae.2022.30.3.293

Impact of adjacent excavation on the response of cantilever sheet pile walls embedded in cohesionless soil

Akshay Pratap Singh[a] and Kaustav Chatterjee*

Department of Civil Engineering, Indian Institute of Technology Roorkee, Roorkee 247 667, India

(*Received September 10, 2021, Revised July 16, 2022, Accepted July 18, 2022*)

Abstract. Cantilever sheet pile walls having section thinner than masonry walls are generally adopted to retain moderate height of excavation. In practice, a surcharge in the form of strip load of finite width is generally present on the backfill. So, in the present study, influence of strip load on cantilever sheet pile walls is analyzed by varying the width of the strip load and distance from the cantilever sheet pile walls using finite difference based computer program in cohesionless soil modelled as Mohr-Coulomb model. The results of bending moment, earth pressure, deflection and settlement are presented in non-dimensional terms. A parametric study has been conducted for different friction angle of soil, embedded depth of sheet pile walls, different magnitudes and width of the strip load acting on the ground surface and at a depth below ground level. The result of present study is also validated with the available literature. From the results presented in this study, it can be inferred that optimum behavior of cantilever sheet pile walls is observed for strip load having width 2 m to 3 m on the ground surface. Further as the depth of strip load below the ground surface increases below the ground level to 0.75 times excavation height, the bending moment, settlement, net earth pressure and deflection decreases and then remains constant.

Keywords: cantilever sheet pile walls; cohesionless soil; embedded depth; FLAC2D; numerical analysis; strip load

1. Introduction

Rapid urbanization places high pressure on infrastructure development resulting in deep excavation projects due to lack of space. The proliferation of high rise buildings and underground spaces in limited areas have placed high pressure on geotechnical engineers to use suitable retaining walls during deep excavations. The use of type of retaining wall depends on the soil stratigraphy and depth of excavation. In general, for small height of excavation about 5 m, flexible cantilever sheet pile walls (CSPW) are used. These sheet piles are used since ancient times but in 20th century engineers started to design based on the variation of earth pressure (Blum 1931, Krey 1936). Terzaghi (1954) presented the uncertainties involved in the previous work and recommended the use of allowable stresses in sheet piling and safety factors in the passive pressures. Previously, Padfield and Mair (1984) and Bowles (2012) suggested the net pressure profiles for CSPW in cohesionless soil which are generally used in current scenarios. El-Emam and Touqan (2020) found out that the load carrying capacity increased and settlement decreased with increase in the distance from the non-yielding wall. For numerical analysis, different techniques like the finite element approach (Day 1999, Bilgin 2010) and finite difference approach (Callisto 2014, Callisto and Soccodato 2010, Chowdhury *et al*. 2016, Conti *et al*. 2014, Conti and Viggiani, 2013, Singh and Chatterjee 2020b, 2020c, 2020d) have also been used to analyze CSPW in static as well as dynamic conditions. Ghadrdan *et al*. (2020) investigated the sensitivity of the stability analysis of a deep excavation in Australia and Nguyen and Likitlersuang (2021) presented a case study to investigate the effects of the spatial variability of a soil's undrained shear strength on the horizotanl wall movements and ground surface settlement. Ahmadi and Ahmadi (2019) presented a case study of a corner of a deep excavation using the 2D and 3D numerical modelling to estimate the wall deflection at the corner locations. Sudani *et al*. (2015) used 3D finite element analysis package ANSYS 13.0 to investigate the bearing capacity of a concrete footing placed near a wall of spaced driven concrete piles. Ahmad *et al*. (2021) carried out experimental and numerical studies on the reinforced and unreinforced cohesionless soils adjacent to excavation loaded with square footings. Ahmad *et al*. (2021) used finite element analysis to suggest the optimal number of reinforcements required to the bearing capacity. Beygi (2021) carried out a numerical study using finite element method to find the effect of variation in the rotational stiffness and wall height on the behaviour of retaining wall. Jao *et al*. (2017) investigated the influence reinforced concrete strip footings placed on the backfill on the reinforced concrete sheet pile walls. El Sawwaf (2010) carried out a laboratory model test and theoretical analysis for the strip footing supported on a sheet pile wall-stabilized sandy slope. Jiang *et al*. (2018) carried out a numerical study using finite element method with Duncan-Chang E-v model to investigate the stress and deformation behavior of sheet pile structure. Capacity spectrum method is used to design the sheet pile retaining

*Corresponding author, Assistant Professor
E-mail: kaustav.chatterjee@ce.iitr.ac.in
[a]Ph.D.
E-mail: asingh4@ce.iitr.ac.in

ISSN: 2005-307X (Print), 2092-6219 (Online)

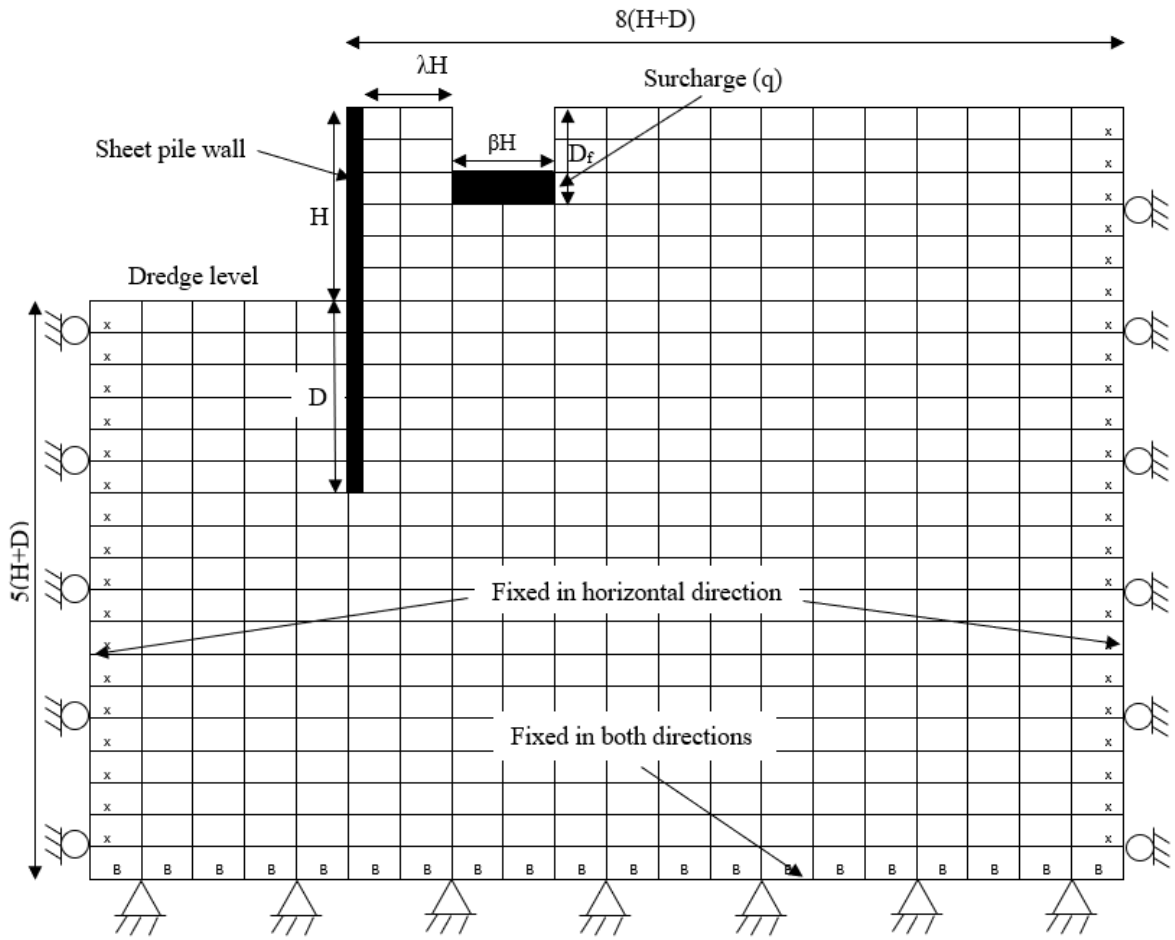

Fig. 1 FLAC2D model used in the present study

wall for seismic application (Qu *et al*. 2016). Doubrovsky and Meshcheryakov (2015) modeled the sheet piles in the laboratory to improve the numerical modeling. Krabbenhoft (2018) described the design of embedded retaining walls by using the plastic limit state approach. Singh and Chatterjee (2021b) improved the rectilinear design of cantilever sheet pile wall considering the surcharge on the backfill and the coefficients of earth pressure derived using lower bound theorem of plasticity. Gazan (2011) developed the normalized relations for calculating the depth of embedment of sheet pile walls in terms of normalized strength of soil in cohesionless soil. Recently, Gaba *et al*. (2017) presented a report on the design of the embedded retaining wall.

However, a surcharge of finite width is generally present on the backfill side of the structure. Caltabiano *et al*. (2012) analyzed the retaining wall for limited as well as infinite surcharge by considering the frictional resistance present below the retaining wall. Similarly, in practice, sheet pile walls are subjected to uniform applied stress of finite width at a distance from the wall. Limited research has been done on sheet pile walls subjected to surcharge loadings. Steenfelt and Hansen (1984) analyzed the sheet pile wall with strip load over the backfill for cohesionless soil analytically using Brinch Hansen's earth pressure theory by following a circular failure arc. Georgiadis and Anagnostopoulos (1998) performed a model test on sheet pile wall to analyze the influence of the surcharge strip on wall behavior and showed that bending moment diagrams by simple 45º load distribution approach and Coulomb analysis matches well with the experimental results. Recently, the design of sheet pile wall considering strip load has been carried out considering partial mobilization (Singh and Chatterjee 2022a) and full mobilization (Singh and Chatterjee 2022b) using the limit equilibrium method.

The earth pressure produced due to the strip load affects the nearby cantilever sheet pile wall which necessitates the efficient design of the wall. The study related to the influence of strip load on the behavior of cantilever sheet pile wall has not been done previously. As the analysis with finite difference approach provides good results (Singh and Chatterjee 2020a, 2020d, 2021a), therefore, in the present study, the influence of smooth strip load placed on the backfill at a distance from the wall on the behavior of CSPW is analyzed in cohesionless soil using finite difference-based computer program FLAC2D.

2. Numerical modeling of cantilever sheet pile walls

2.1 The software environment

It is true that three-dimensional numerical simulation gives accurate results. The over estimation of contact area

Table 1 Properties of sheet pile walls considered in the present study (Nucor Skyline 2017)

Type	Cross Section Area (cm^2/m)	Section Modulus (cm^3/m)	Moment of Inertia (cm^4/m)	Elasticity Modulus (kN/m^2)	Stiffness (kNm^2/m)
SKZ 38	234.4	3350	76588	2.03×10^8	1.6×10^5

Table 2 Soil properties considered in the present study (Bowles 2012, Singh and Chatterjee 2021a)

Soil type	Properties			
	Angle of internal friction (φ)	Poisson's ratio (μ)	Modulus of elasticity (E) in MPa	Unit weight (γ) in kN/m^3
Dense sand	39°	0.30	90	18.4
Medium sand	34°	0.34	65	16.0
Loose sand	30°	0.38	36	14.0

and specific radiation damping per unit contact area in two-dimensional case does not recommend it to apply in practice (Wolf and Song 2002). Further, a correction is applied to the results of FLAC2D to obtain the better results as available in FLAC3D (Hazzar *et al*. 2020). However, to simplify the soil-structure interaction analysis and availability of limited software, two-dimensional finite-difference based computer program FLAC 2D (Itasca 2016) is used in the present study to model the CSPW with strip load by considering the plane strain problem (Hsiung *et al*. 2021).

2.2 Model setup

The model dimensions considered for width of backfill and depth below excavation level are 8(H+D) and 5(H+D) respectively (Singh and Chatterjee 2020d). The domain size and boundary conditions for the present study are shown in Fig. 1. The width of the excavation is taken as 15 m. The cohesionless soil is assumed to be fully dry. The modeling is completed in two steps, i.e., wall installation and excavation. The CSPW with properties tabulated in Table 1 are installed in the soil domain having properties tabulated in Table 2 and then excavation is carried out each with 1 m level.

2.3 Boundary conditions

Vertical boundary nodes are restricted to move in a horizontal direction and allowed in a vertical direction. Further, bottom boundary nodes are restricted to move both in horizontal as well as vertical directions. The interaction of soil with the wall in FLAC 2D is represented by normal stiffness (K_n) and shear stiffness (K_s), the value of which is 10 times the equivalent stiffness of the stiffest neighboring zone. The equivalent stiffness of the stiffest neighboring zone is given in Itasca (2016) as

$$\text{Equivalent stiffness}=\left(\frac{K+\frac{4}{3}G}{\Delta z_{\min}}\right) \quad (1)$$

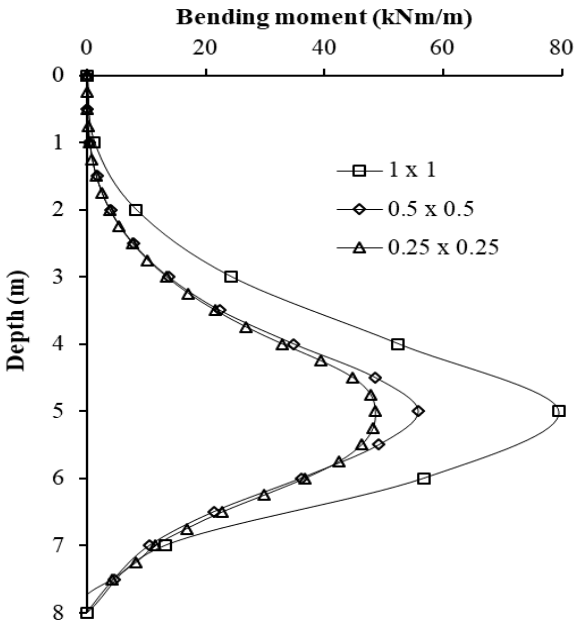

Fig. 2 The influence of mesh size dimensions in meter on bending moment results of CSPW

where K, G and $\Delta z_{\min}$ being the bulk modulus, shear modulus and smallest width of the adjoining zone in the normal direction to the interface. Thus, normal stiffness (K_n) and shear stiffness (K_s) are given as

$$K_n=K_s=10\times\left(\frac{K+\frac{4}{3}G}{\Delta z_{\min}}\right) \quad (2)$$

2.4 Constitutive law

The stress-strain behavior of the soil is modeled as a two-part model, i.e., elastic-perfectly plastic Mohr-Coulomb model and sheet pile walls are modeled using beam elements.

2.5 Mesh size

For determining the influence of mesh size on the certainty of numerical results, an analysis is carried out with mesh size 1 m×1 m, 0.5 m×0.5 m and 0.25 m×0.25 m. The model dimensions considered for width of backfill and depth below excavation level are 8(H+D) and 5(H+D) respectively (Singh and Chatterjee 2020d). It is well known that the finer the mesh, the better is the accuracy of results. The bending moment distribution of the CSPW as a result of the analysis is presented in Fig. 2. According to Fig. 2, mesh size of dimensions 1 m×1 m, 0.5 m×0.5 m and 0.25 m×0.25 m have similar variations along the depths and the difference in the maximum value of bending moment are less for mesh dimensions 0.5 m×0.5 m and 0.25 m×0.25 m. Therefore, considering the time consumed in the analysis and the availability of computer configuration, in the present study, mesh size 0.5 m×0.5 m are considered for the analysis.

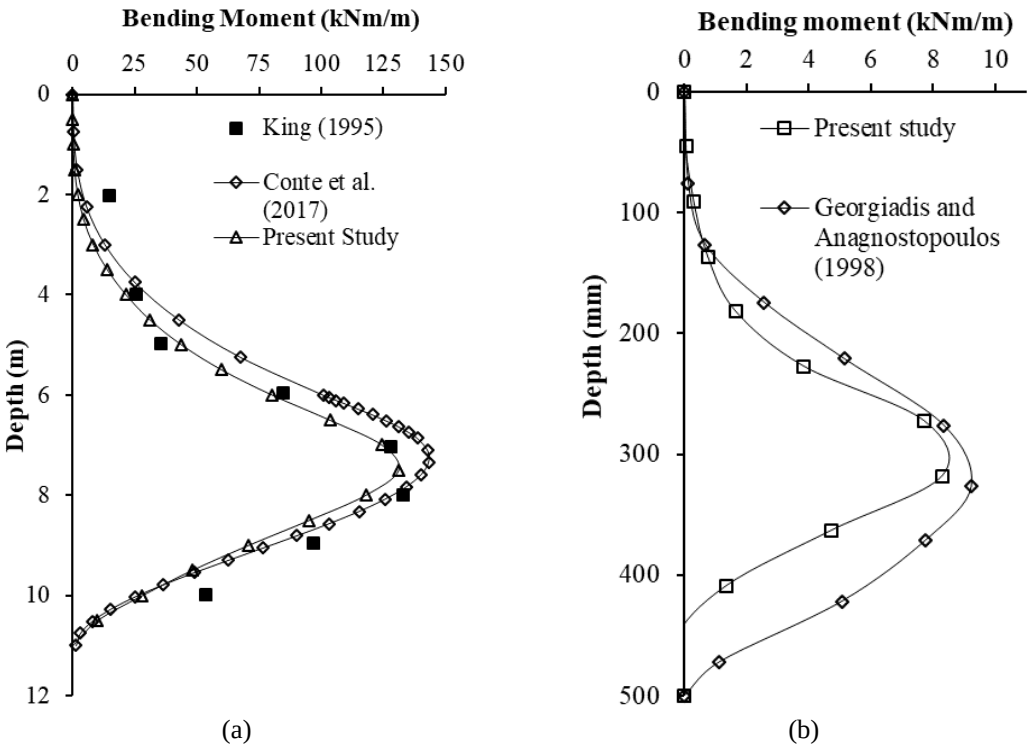

Fig. 3 Comparison of bending moment along depth obtained in the present study with that of (a) King (1995) and Conte *et al*. (2017) for no surcharge, (b) Georgiadis and Anagnostopoulos (1998) for q=12 kPa

3. Validation of the present numerical model

3.1 Validation with bending moments

The bending moment results of cantilever sheet pile wall obtained through the present numerical model are compared with King (1995) and Conte *et al*. (2017) for no surcharge condition and Georgiadis and Anagnostopoulos (1998) for strip load q=12 kPa.

For no surcharge condition, a cantilever sheet pile wall with excavation height of 6 m and embedded depth of 5 m is assumed in the sand with γ=14.2 kN/m^3, ϕ=40° and δ=15.8° (King 1995). The comparison of bending moment results along the depth for King (1995), Conte *et al*. (2017) and the present numerical model are illustrated in Fig. 3(a). It is observed that the variation of bending moment along the depth are comparable.

For the surcharge condition, the results of the model test conducted by Georgiadis and Anagnostopoulos (1998) are used to validate the present numerical model. A 500 mm long CSPW (H=250 mm and D=250 mm) made of aluminum alloy of Young's modulus (E) 70 GPa is installed in the soil having γ=15.5 kN/m^3, ϕ=42° and subjected to a surcharge in the form of strip load q=12 kN/m^2 applied over the 100 mm length of backfill at a distance of 250 mm from the top of the wall by Georgiadis and Anagnostopoulos (1998) and the same is simulated in FLAC2D. A comparison of variation of bending moment along the depth of the sheet pile wall is made by plotting the results for both the present numerical method as well as model tests by Georgiadis and Anagnostopoulos (1998) as shown in Fig. 3(b). Good conformity is observed between the result of the present numerical model and Georgiadis and Anagnostopoulos (1998).

Therefore, it is confirmed that the present numerical model can be used to analyze the cantilever sheet pile wall with strip load. The slight variation between the two curves may be due to errors involved in the performing experiments and the properties (Young's modulus and Poisson's ratio) taken in FLAC2D.

3.2 Validation with deflection

The deflection of cantilever sheet pile wall obtained through the present numerical model is compared with Aparna and Samadhiya (2019) for strip load q=20 kPa. The results of the model test conducted by Aparna and Samadhiya (2019) are used to validate the numerical model. A 750 mm long CSPW (H=300 mm and D=450 mm) made of galvanised iron is installed in the soil having ϕ=34°, coefficient of curvature (C_c)=0.84, coefficient of uniformity (C_u)=1.62 and specific gravity (G_s)=2.67 and subjected to a surcharge in the form of strip load q=20 kPa applied over a length of 150 mm of the backfillat a distance of 200 mm from the top of the wall by Aparna and Samadhiya (2019) and the same is simulated in FLAC2D. A comparison of the variation of deflection along the depth of the sheet pile is made by plotting the results for both the present numerical model as well as model test by Aparna and Samadhiya (2019) as shown in Fig. 4. It is observed that the result of the present numerical model and Aparna and Samadhiya (2019) matches well.

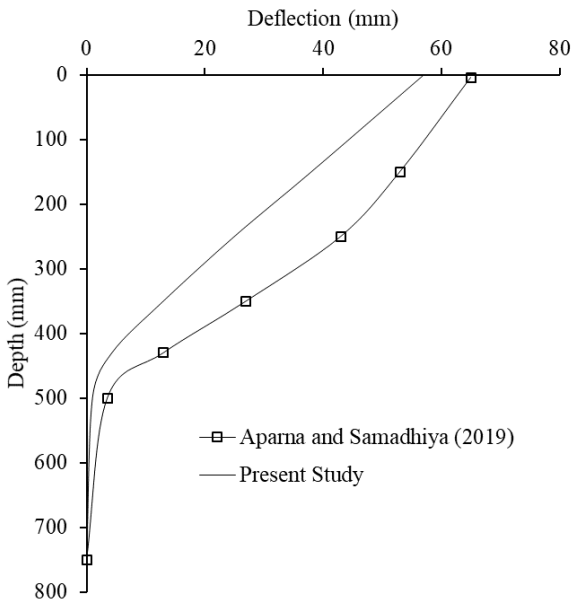

Fig. 4 Comparison of deflection along the depth obtained in the present study with that of Aparna and Samadhiya (2019)

Table 3 Different input parameters considered in the present study

Parameters	Values
Magnitudes of uniform surcharge loading (q) in kPa	20, 50 and 100
Distance of uniform surcharge load from the top of the wall (λH) in m	0, 1, 2, 3, 4, 5, 6, 8 and 12
Height of excavation (H) in m	2, 4, 6, 8
Embedded depths (D) in m	2, 4, 6, 8 and 10
Angle of internal friction	ϕ=30°, ϕ=34° and ϕ=39°

4. Present study

After validation of the numerical model, a parametric study is carried out for the flexible CSPW with varying normalized width (β), magnitude (Q) of strip load and its normalized distance from the top of the wall (λ) in the dry homogeneous and isotropic soil layer. The normalized width of strip load, β, and normalized distance from the

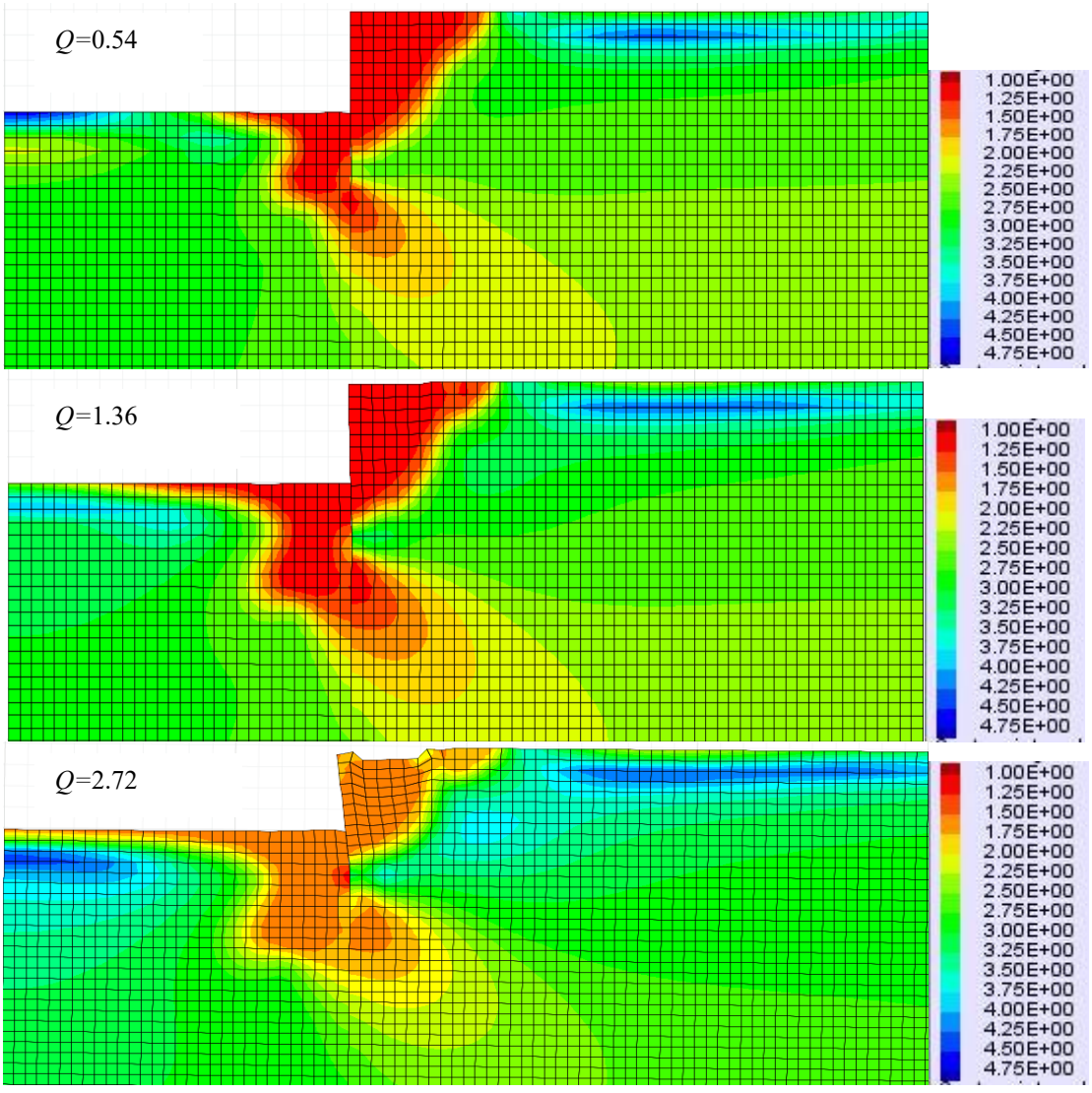

Fig. 5 Mohr Coulomb Strength/Stress ratio for cantilever sheet pile wall (H=4 m and D=2 m) having strip load of β=0.5 and λ=0.25 in dense sand

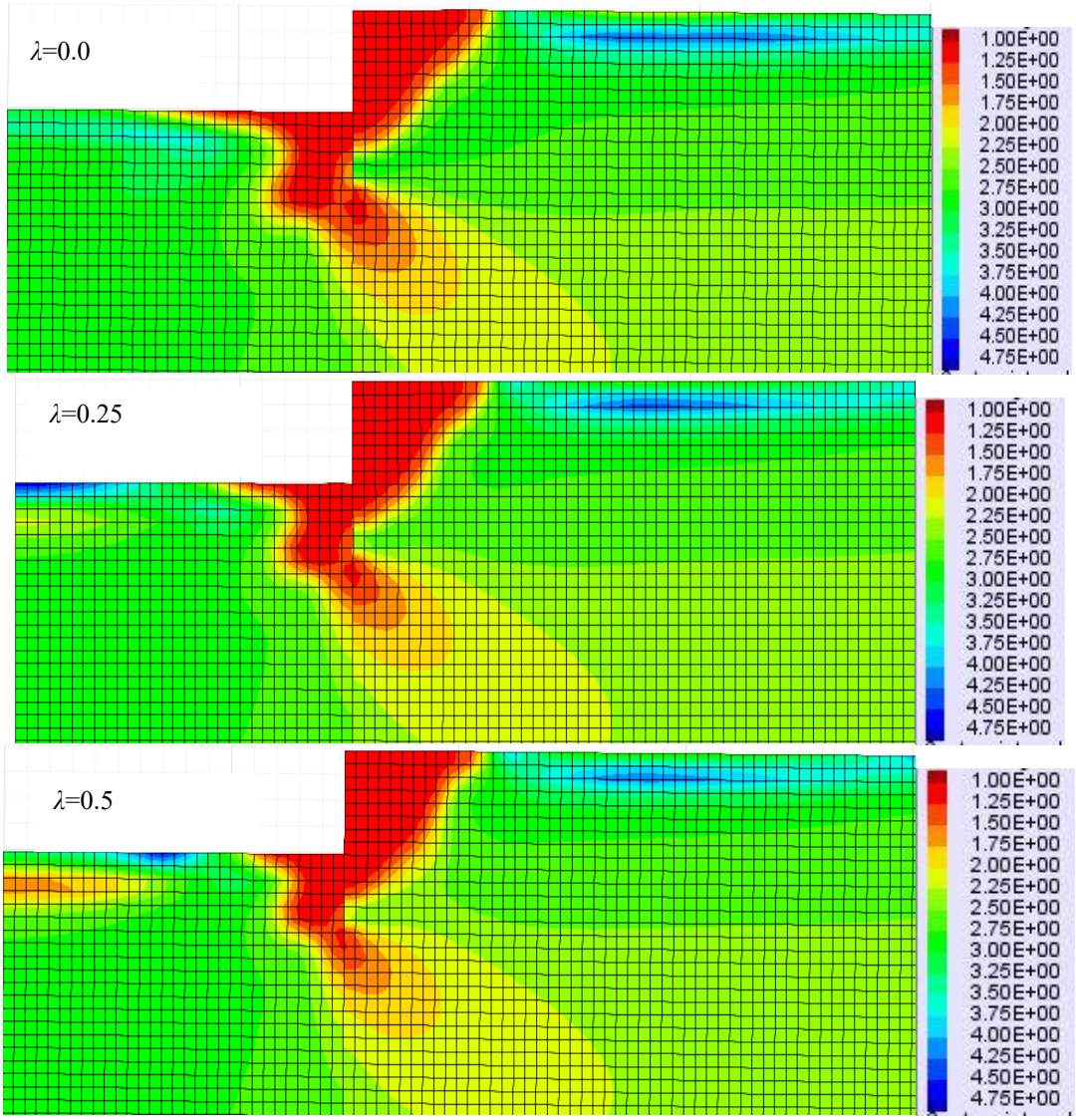

Fig. 6 Mohr Coulomb Strength/Stress ratio for cantilever sheet pile wall (H=4 m and D=2 m) having strip load of β=0.5 and Q=0.54 in dense sand

wall (λ) are defined as the ratio of the width of strip load (b) to excavation height (H) and distance of surcharge from the wall (a) to excavation height (H) respectively. For all the parametric studies, height (H) and width of excavation are assumed constant as 4 m and 15 m respectively. The magnitude of the strip load is normalized with respect to $\gamma H/2$ and represented as Q. The width of strip load, its distance from the wall, friction angle (at constant soil-wall friction angle $\delta=2\phi/3$), the magnitude of strip load present on the ground surface and at a depth below the ground level assumed for the present study are tabulated in Table 3. The properties of the three types of sand used are tabulated in Table 2. The results obtained in the present study are presented in non-dimensional terms as normalized bending moment, earth pressure, deflection and settlement.

5. Results and discussions

In the present section, results of the influence of distanced strip load on the bending moment, earth pressure, deflection and movement of the ground surface are presented.

5.1 Influence of distanced strip load on Mohr-Coulomb Strength/Stress ratio

The mechanism of CSPW can be understood with the help of the Mohr-Coulomb Strength/Stress ratio. Fig. 5 illustrates the Mohr-Coulomb Strength/Stress ratio for CSPW (H=4 m and D=2 m) having a strip load Q=0.54, 1.36 and 2.72 of β=0.5 and λ=0.25 in dense sand. Mohr-Coulomb Strength/Stress ratio represents shear strength of the soil divided by the particular shear stress, which means the soil near the cantilever sheet pile wall has attained the shear strength and the soil away from the cantilever sheet pile wall is still under less stress than the shear strength. It is observed that as the magnitude of strip load increases from Q=0.54 to 1.36, the stress in the passive zone is more mobilized but for Q=2.72, the CSPW fails. The failure of

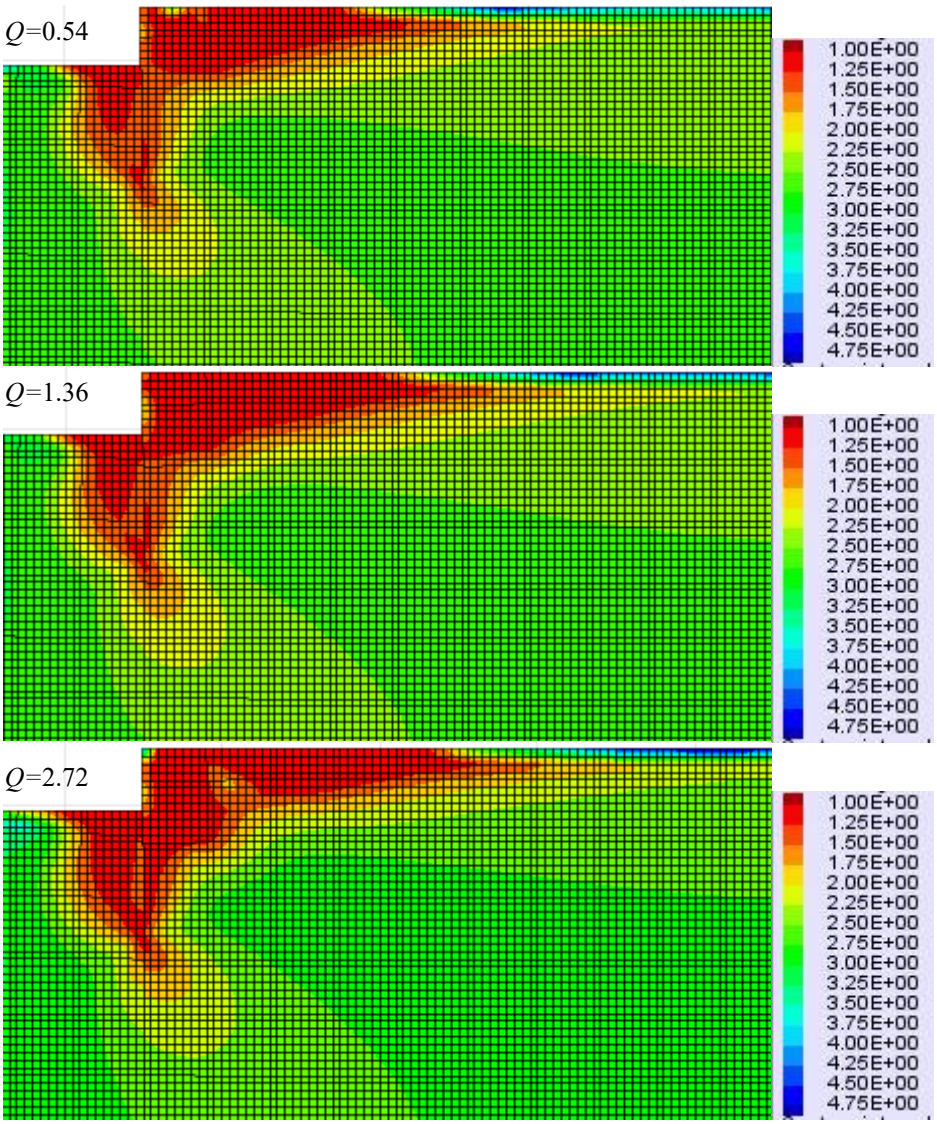

Fig. 7 Mohr Coulomb Strength / Stress ratio for cantilever sheet pile wall (H=4 m and D=8 m) having strip load of β=0.5 and λ=0.25 in dense sand

the cantilever sheet pile wall is due to inadequate embedded depth which could not sustain the increased earth pressure due to increment of the magnitude of the strip load. Fig. 6 illustrates the influence of distance of strip load (λ) from CSPW (H=4 m and D=2 m) in dense sand for Q=0.54 and β=0.5. It is observed that as λ increases, the mobilization of the stress in the passive zone gets reduced as the influence of strip load on CSPW decreases. The reduction in mobilization of stress can be easily understood with the Mohr-Coulomb Strength/Stress ratio as discussed before in this section.

The influence of strip load on the increase in embedded depth to D=8 m and H=4 m in dense sand has been shown in Figs. 7 and 8 for different magnitudes of strip load and distance from the sheet pile wall. Fig. 7 also illustrates the more mobilization of stress with an increase in the magnitude of the surcharge load. Further, from Fig. 8 it is clearly observed that when the strip load is near CSPW, more mobilization of stress takes place in the active zone on the backfill side and vice versa.

5.2 Influence of distanced strip load on bending moment

The influence of strip load present on the backfill of the sheet pile wall is analyzed and the results are presented in the form of normalized maximum bending moment ($M_{max}/\gamma H^3$) in percentage. Fig. 9 highlights the influence of the width of strip load in terms of strip width ratio (β) for different distances from the wall (λ) at normalized strip load Q=0.54 and D/H=1 in dense sand. It is observed that for narrow strip load, the maximum bending moment increases significantly while small variations are observed for wider strip load. The maximum normalized bending moment is observed for strip load placed at the top of the wall (λ=0) of strip width ratio (β) 0.5 and 0.75 as 7.44% and 7.48% respectively. As the strip load is placed away from the top of the wall λ=0.25, 0.5, 0.75, 1, 1.5 and 2, the maximum normalized bending moment for β=0.5 decreases as 5.6%, 5.08%, 4.94%, 4.87%, 4.84% and 4.84% respectively. The normalized maximum bending moment for increasing λ is

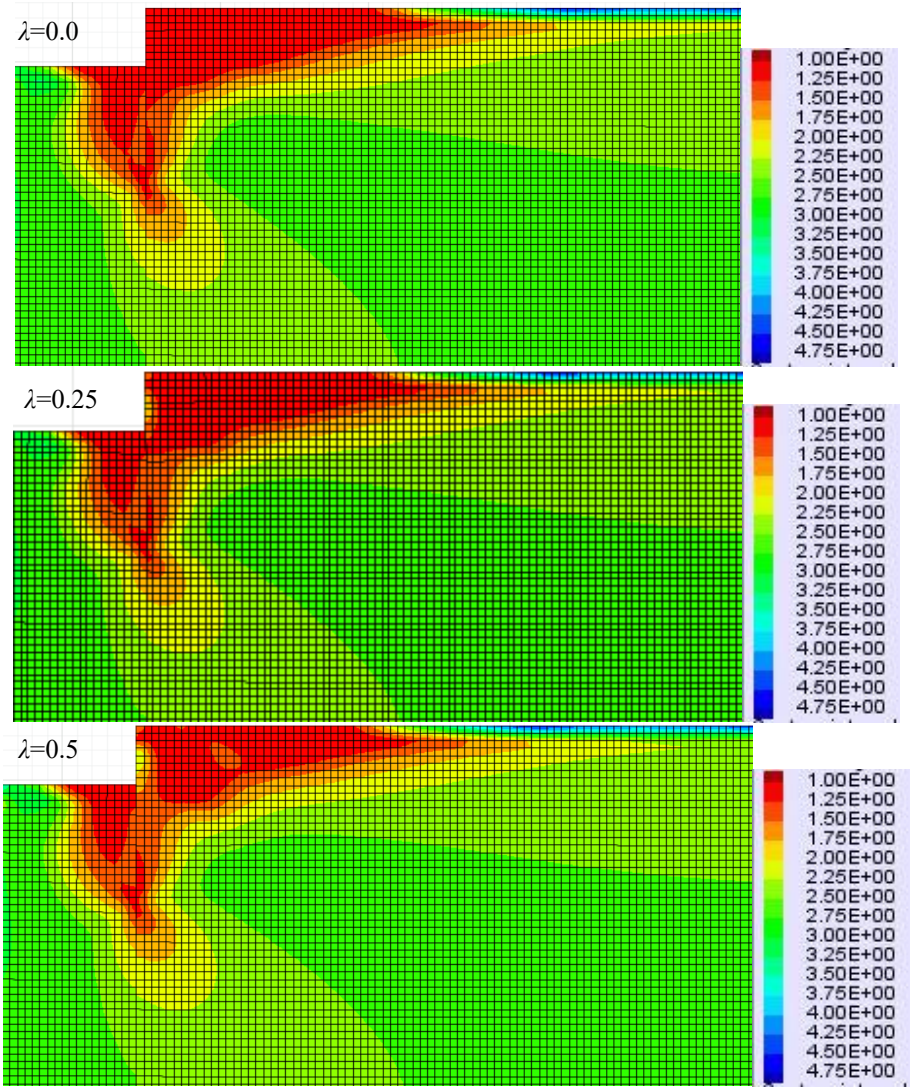

Fig. 8 Mohr Coulomb Strength / Stress ratio for cantilever sheet pile wall (H=4 m and D=8 m) having strip load of β=0.5 and Q=1.36 in dense sand

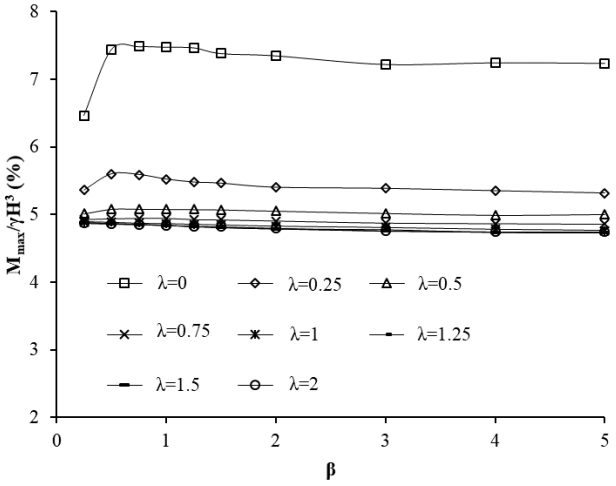

Fig. 9 Variation of normalized bending moment with β for different λ at Q=0.54 and D/H=1 in dense sand

decreasing up to λ=0.75 and then becomes constant. As the maximum normalized bending moment without strip load is 4.82%, thereby the maximum increase in bending moment observed after placing the strip load at λ=0 and 0.25 are 54.3% and 16.2% respectively. Though, for λ=0, strip load develops more pressure than any other strip position, λ=0.25 is considered in the present study as the load will be at a distance from the excavation. Therefore, the strip load of strip width ratio (β) 0.5-0.75 at λ=0.25 can be considered most effective for analysis.

Furthermore, the change in behavior of CSPW is also observed for different embedded depths as the distance of strip load increases away from the wall as shown in Fig. 10. If the load is near the top of the sheet pile wall (λ=0 and 0.25), the normalized maximum bending moment observed for D/H=0.5 is less than D/H=1, 1.5 and 2 for different width of strip load and the trend for D/H=1 shifts towards D/H=0.5 as the distance of strip load increases. Thus, the behavior of CSPW is divided into two parts based on embedded depth for $\lambda \geq 0.5$. The variation of the normalized maximum bending moment for $D/H \leq 1$ and $D/H \geq 1.5$ are different and approximately constant for $\lambda \geq 0.5$. It clearly shows that the behavior of sheet pile wall depends on the

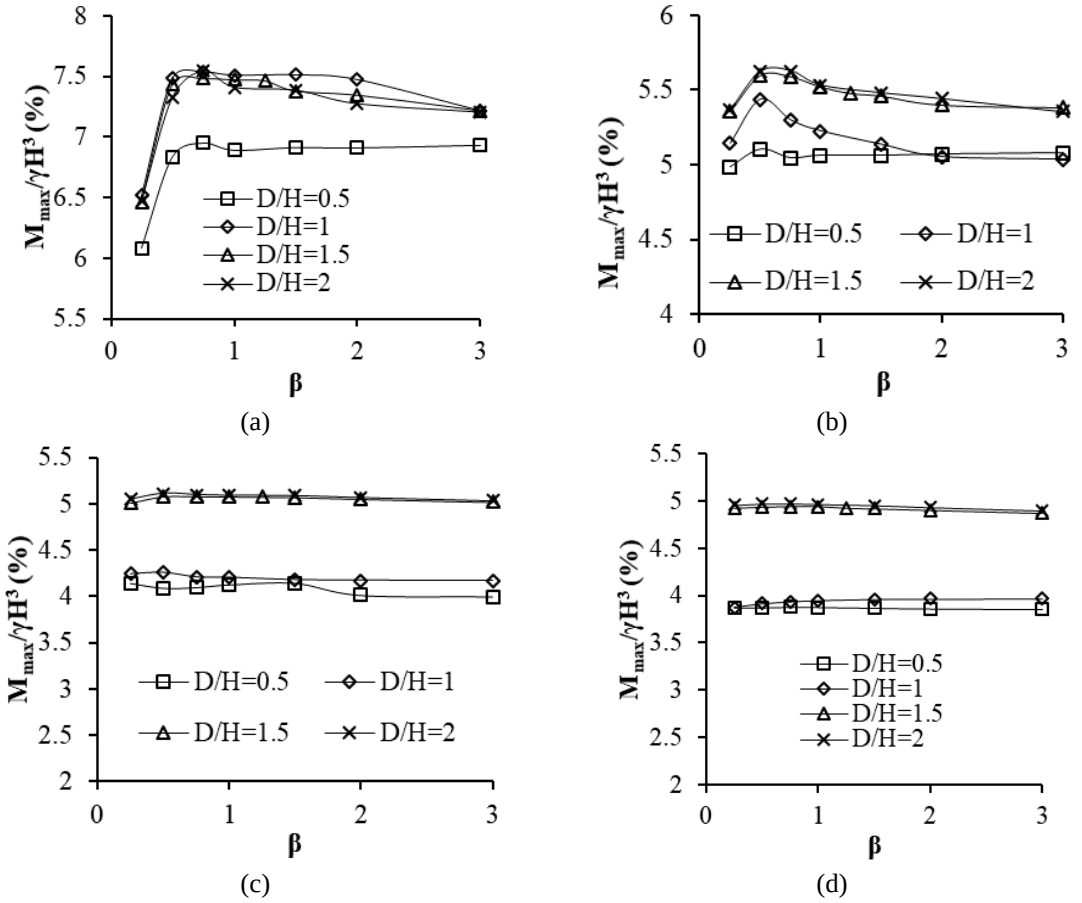

Fig. 10 Influence of embedded depth on normalized bending moment with β for (a) λ=0, (b) λ=0.25, (c) λ=0.5 and (d) λ=0.75

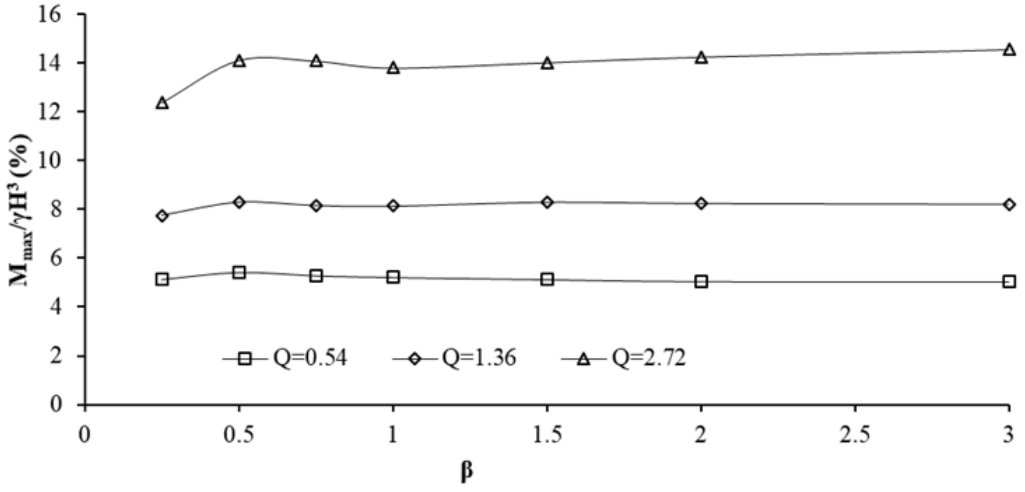

Fig. 11 Variation of normalized bending moment with β for different magnitude of strip load at λ=0.25

embedded depth significantly.

The influence of the magnitude of surcharge for various widths of strip load at λ=0.25 is highlighted in Fig. 11. The vertical pressure applied on the backfill, which increases on the application of higher magnitude of strip load, increases the lateral pressure and thus to satisfy the equilibrium condition, more normalized maximum bending moment is observed with high magnitude of strip load. Also, for all magnitudes of surcharge, the maximum normalized bending moment observed is maximum near about β=0.5. Furthermore, the resistance capacity of sand particles present adjacent to the structure also affects the behavior of the structure. The resistance capacity in the sand having a high friction angle is high as compared to sand having low friction angle. Therefore, the bending moment requirement of sheet pile wall in sand having a high friction angle is less when compared with sand of low friction angle as shown in Fig. 12.

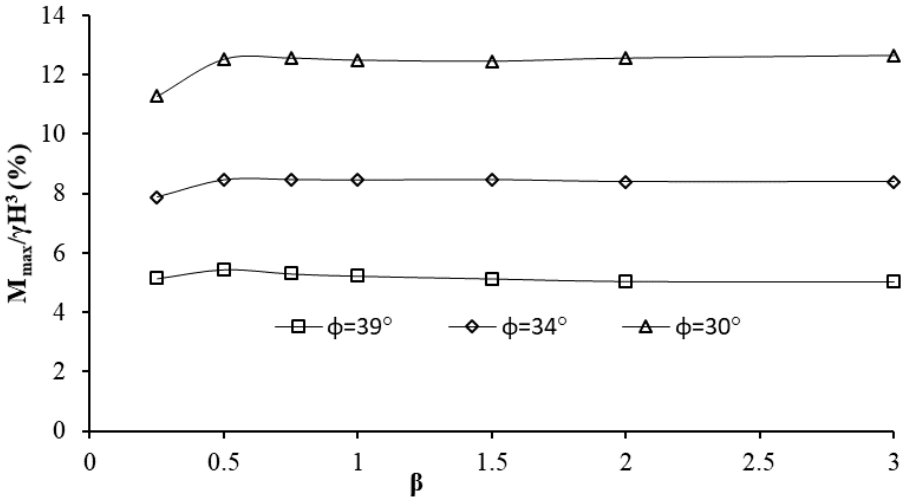

Fig. 12 Influence of different friction angle of sand on normalized bending moment with β at λ=0.25 with D/H=1

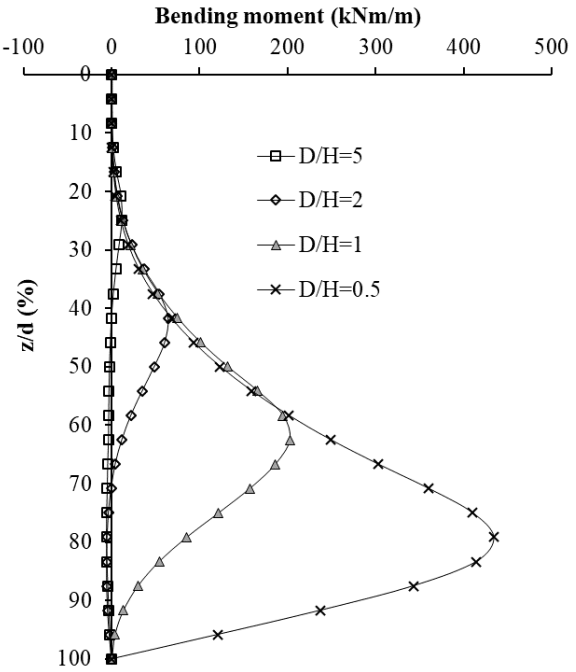

Fig. 13 Influence of different excavation height of CSPW on normalized bending moment along the depth with λ=0.25 and β=0.5 in dense sand

The influence of different excavation height of the CSPW on the bending moment along the depth with Q=0.54, λ=0.25 and β=0.5 are shown in Fig. 13. The total depth of the CSPW is kept constant as 12 m and excavation heights are altered and correspondingly the embedded depths are also changed. It is observed from Fig. 13 that when D/H=5 (i.e., H=2 m and D=10 m), the imbedded depth is more than sufficient and the maximum bending moment observed is 11.44 kNm/m and with the increase in the height of excavation as D/H=2, 1 and 0.5, the maximum bending moment increases as 65, 202 and 434 kNm/m respectively. When the height of excavation is small, the lateral passive resistance to provide stability to the CSPW is less developed which results in the less maximum bending moment. Further, as the height of excavation is increased, the lateral passive resistance is developed more to provide stability to the CSPW and hence the maximum bending moment increases.

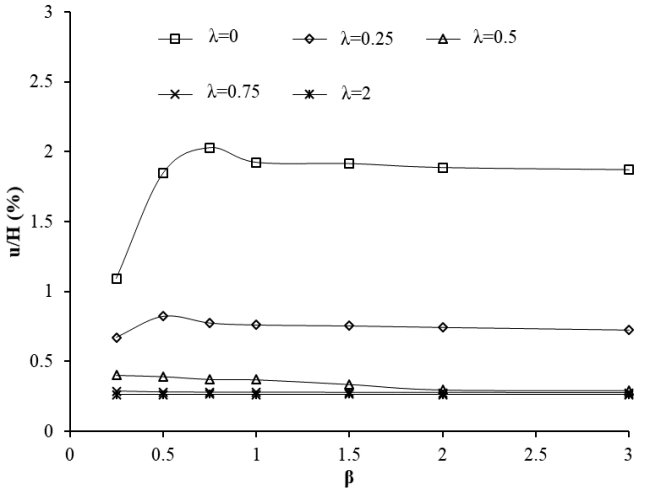

Fig. 14 Variation of normalized deflection with β for different λ at Q=0.54 and D/H=0.5 in dense sand

5.3 Influence of distanced strip load on the deflection

The existence of strip load on the backfill of CSPW is crucial in terms of deflection. The deflection of the sheet pile wall must be within the permissible limit so as not to cause any harm to the existing building. The values of deflection (u) are normalized with respect to excavation depth (H) and depth (z) is normalized with respect to the total length of sheet pile walls (d) and expressed as u/H and z/d in percentage. Fig. 14 shows the variation of deflection of CSPW with respect to strip width ratio for varying distance from the top of the wall for normalized strip load Q=0.54 and D/H=0.5 in dense sand. It is observed that when the strip load is at the top of the wall (λ=0), maximum normalized deflection (2.03%) is observed at β=0.75. However, the increase in distance between CSPW and strip load generates the maximum normalized deflection at β=0.5. Reduction in maximum deflection of CSPW is

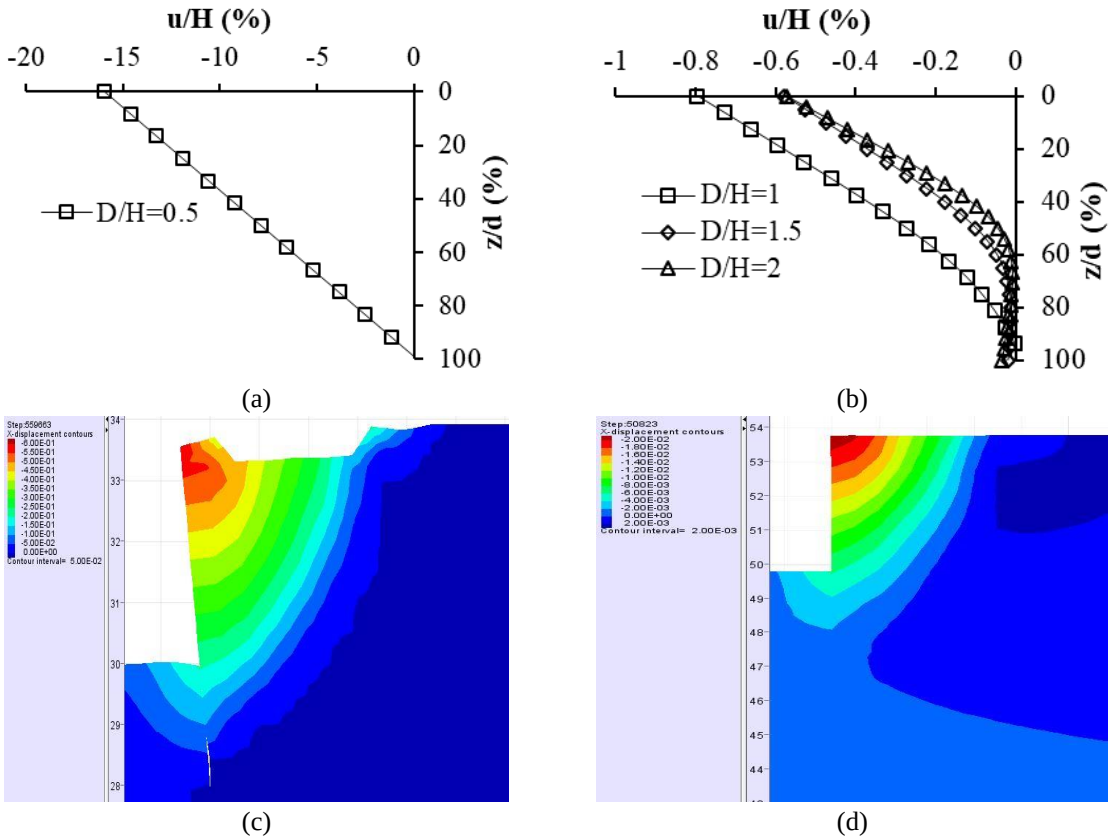

Fig. 15 Deflection behavior of CSPW for different *D/H* at β=0.5, λ=0.25 and Q=2.72 in dense sand (a) *D/H*=0.5 (b) *D/H*=1, 1.5 and 2 and horizontal displacement contours for (c) *D/H*=0.5 and (d) *D/H*=1.5

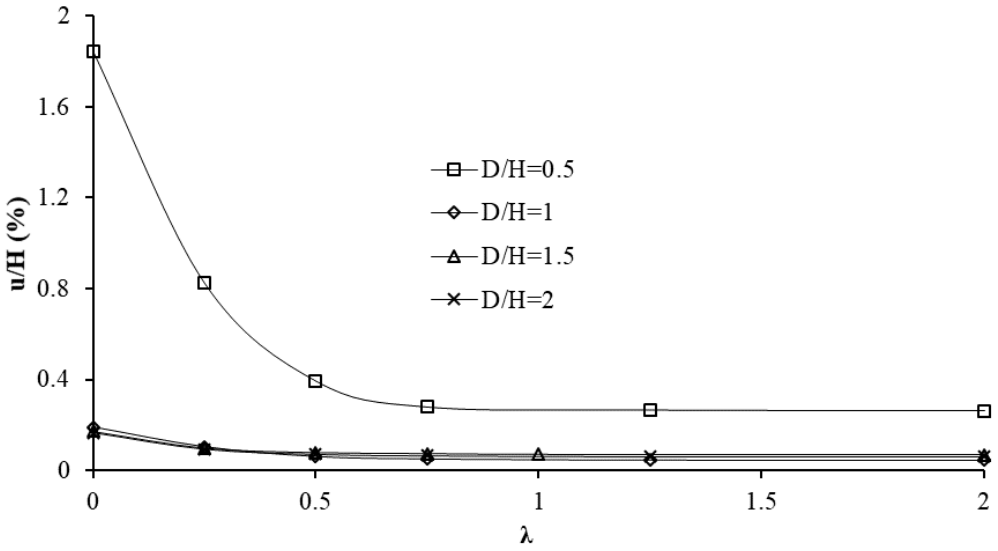

Fig. 16 Variation of normalized deflection with λ for different *D/H* in dense sand at β=0.5

59.3% and 52.3% when strip load is shifted to λ=0.25 and 0.5 from λ=0. Thus, near the sheet pile walls, the width of the strip load influences the deflection of CSPW significantly. There is 85.7% increase in the normalized deflection of CSPW for λ=0, when the strip width ratio increases from β=0.25 to 0.75 and then decreases. The percentage increase is reduced to 23% for λ=0.25 when β increases from 0.25 to 0.5. Beyond λ=0.5, no significant influence of strip width is observed on the deflection.

The deflection behavior of CSPW corresponding to different embedded depth ratio is observed as shown in Fig. 15 for β=0.5, λ=0.25 and Q=2.72 in dense sand where the normalized deflection of CSPW is plotted along with the normalized depth of the wall. For *D/H*=0.5, the sheet pile wall is on the verge of instability and on increasing the embedded depths, CSPW becomes stable in the same cohesionless soil. Furthermore, the deflection observed at top of the wall for *D/H*=0.5 is 15.94% while a significant

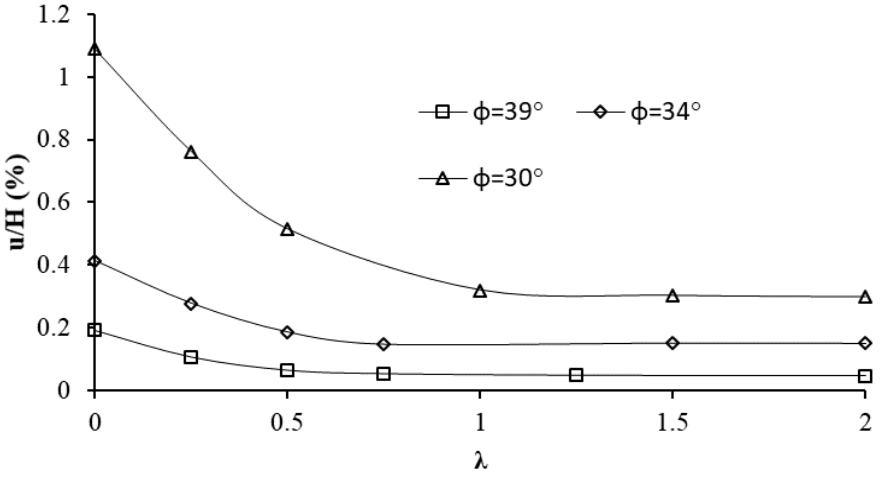

Fig. 17 Effect of different sand on deflection with λ at q=20 kPa, D/H=1 and β=0.5

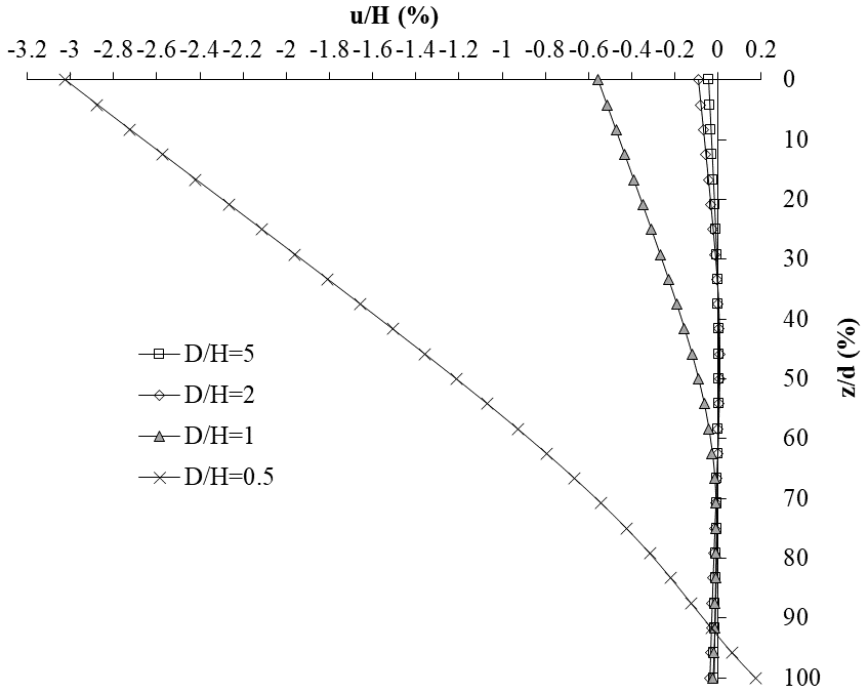

Fig. 18 influence of different height of excavation of CSPW on deflection with Q=0.54, λ=0.25 and β=0.5 in dense sand

reduction is observed for D/H=1, 1.5 and 2 as 0.8%, 0.577% and 0.573% respectively. The significant reduction in the horizontal displacement can also be seen from horizontal displacement contours as shown in Fig. 15(c) and 15(d). The contour diagrams show that for D/H=0.5, the tilting of the sheet pile wall is observed and significant displacement is near the toe of the wall while for D/H=1.5, no tilting is observed and less displacement is observed along the wall. The significant deflection for CSPW having D/H=0.5 is due to less lateral passive pressure present along with the embedded depth and as the lateral passive pressure increases, the deflection decreases and the cantilever sheet pile wall becomes stable.

Fig. 16 highlights the influence of embedded depth on a deflection for Q=0.54 placed at a distance from the wall and β=0.5 in dense sand. The increase in distance between CSPW and strip load from λ=0 to 0.75 for D/H=0.5, 1, 1.5 and 2 decreases the deflection by more than 60% and then remains approximately constant. The deflection for D/H=0.5 is observed high but the behavior for all embedded depths are similar. It clearly shows that the influence of strip load is negligible at a larger distance away from the wall.

The behavior of CSPW for different types of sand is shown in Fig. 17 for q=20 kPa, D/H=1 and β=0.5. It is highlighted in Fig. 17 that at λ=0, the increase in the normalized observed deflection are 117% and 164% for ϕ=34° and ϕ=30° from ϕ=39° respectively. Further, as the distance between the wall and strip load increases, the deflection becomes lesser and beyond λ=1, remains constant.

The effect of different excavation height of the CSPW on the normalized deflection along the depth with Q=0.54, λ=0.25 and β=0.5 are shown in Fig. 18. It is observed from

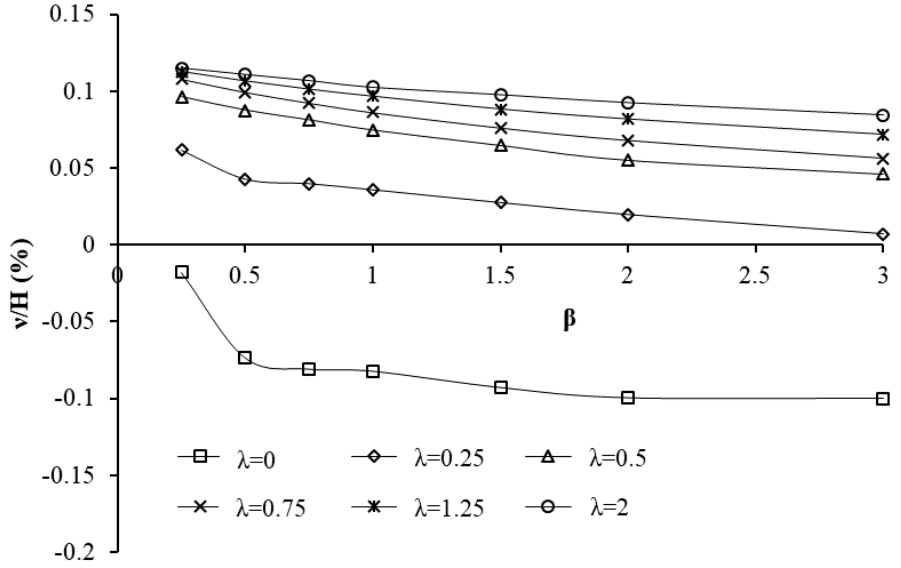

Fig. 19 Variation of ground surface movement with β for different λ at Q=0.54, D/H=1 in dense sand

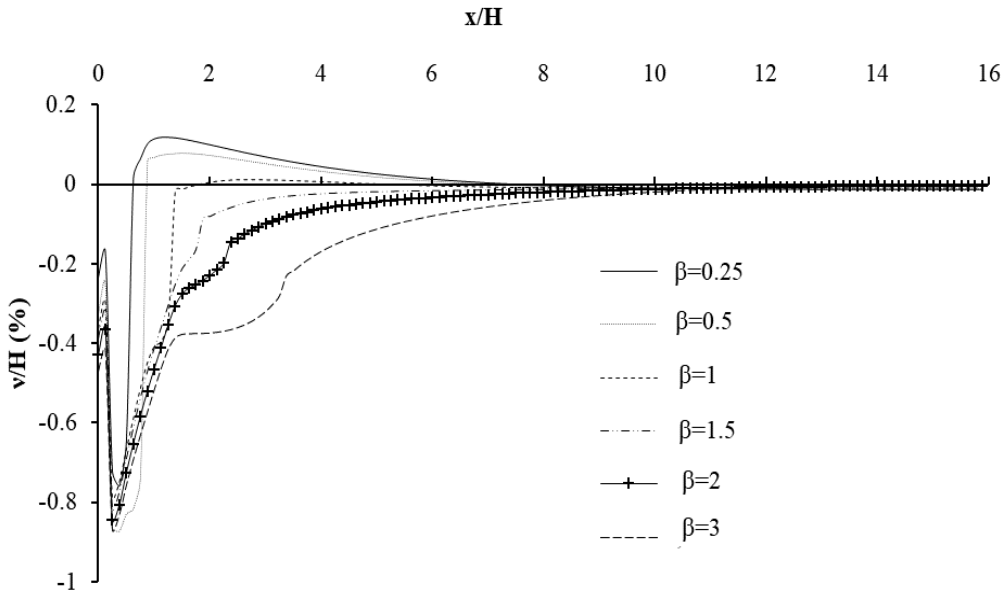

Fig. 20 Profile of ground surface movement for various β at λ=0.25, Q=2.72 and D/H=1 in dense sand

Fig. 18 that when the excavation height of CSPW is increased as D/H=5, 2, 1 and 0.5, the deflection at the top of the CSPW is also increased as u/H=0.045, 0.085, 0.055 and 3.02 % respectively. This is because when the excavation height is less, the lateral earth resistance developed below the dredge level is very less and the CSPW is stable and as the height of excavation is increased, the more lateral earth resistance is required to stable the CSPW and it results in the increase in deflection. It is clearly observed that when D/H=0.5.

5.4 Influence of distanced strip load on the movement of the ground surface

The movement of the ground surface adjacent to CSPW must be assessed before excavation to safeguard the structure from collapse. The retaining structure should be such that during and after excavation, the movement of the ground surface does not harm the structure. Knowing this fact, the ground surface movement is analyzed for various strip width ratio (β) and the distance between the wall and strip load (λ). The values of ground surface movement are normalized with respect to excavation depth (v/H) in percentage and distance from the wall is normalized with respect to excavation depth (x/H). Here, the term maximum ground surface movement is understood as the ground surface movement adjacent to the wall top. Fig. 19 shows the variation of normalized ground surface movement (v/H) in percentage with respect to strip width ratio (β) for different λ at Q=0.54 and D/H=1. The settlement is only observed when the strip load is placed on the top of the wall and at any other position only heaving has occurred. This is because the strip load forms a pressure bulb below the ground surface such that adjacent to the strip load below the

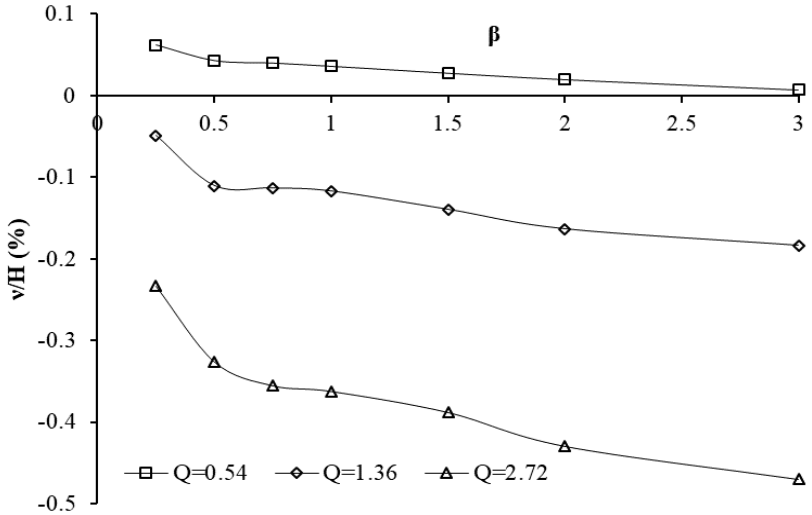

Fig. 21 Variation of normalized ground surface movement with β for different magnitude of strip load at λ=0.25 with D/H=1 in dense sand

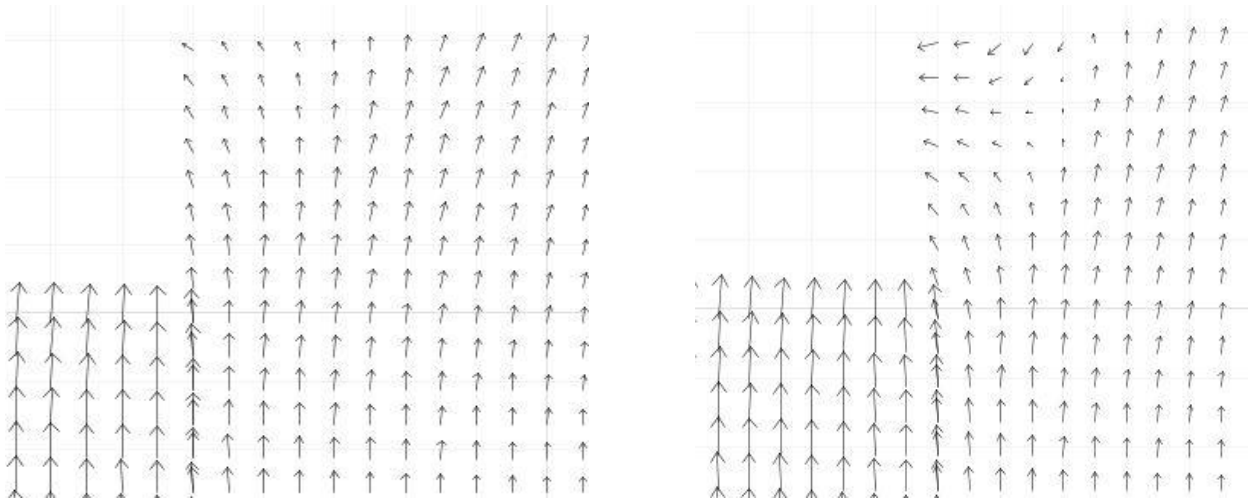

(a) (b)

Fig. 22 Displacement vectors in model for λ=0.25, β=0.25 and D/H=1 for (a) Q=0.54 (b) Q=1.36

ground surface, there is no compressive pressure from the surcharge and it gets heaved due to an increase in lateral stress. The increase in the strip width ratio increases the pressure bulb dimension and hence decreases the heaving as the stress is mobilized to a greater area. It is also observed that settlement of ground surface decreases and heaving takes place as λ increases due to a decrease in surcharge induced lateral earth pressure.

Fig. 20 highlights the profile of ground surface movement along the length of backfill at λ=0.25, Q=2.72, D/H=1 for various width of strip load. The normalized distance from the sheet pile wall is represented as x/H where x is the distance from the sheet pile wall. It is observed that for narrow strip load, the ground surface settles abruptly, forming heave on the backfill while for wider strip load, the ground surface settles smoothly without heaving. The distribution of movement of the ground surface generally extends to a distance of 6H to 8H from the excavation wall. The maximum settlement of ground surface adjacent to sheet pile and below the strip load is less than 0.5% H and 0.9% H respectively while the maximum heaving observed is about 0.1% H. Also, one end near the sheet pile wall is observed to be more settled than the other end. Fig. 21 highlights the influence of the magnitude of strip load on the ground surface movement with respect to strip width ratio (β) at λ=0.25 and D/H=1. The ground surface settlement for normalized strip load Q=0.54, 1.36 and 2.72 are 0.043%, -0.11% and -0.326% respectively for β=0.5. The minus and plus sign refer to the ground surface movement below ground level and heaving occurring adjacent to the wall. It is observed that placement of low magnitude of strip load induce heaving of sand while the settlement is occurred due to placement of high magnitude of strip load. This can be understood by observing the displacement vectors of sand, i.e., pointing of arrow upwards and outwards seen in Fig. 22(a) for Q=0.54 reflects the ground surface heaving and pointing of arrow downwards and outwards seen in Fig. 22(b) for Q=1.36 reflects the ground surface settlement.

The ground surface movement also depends on the

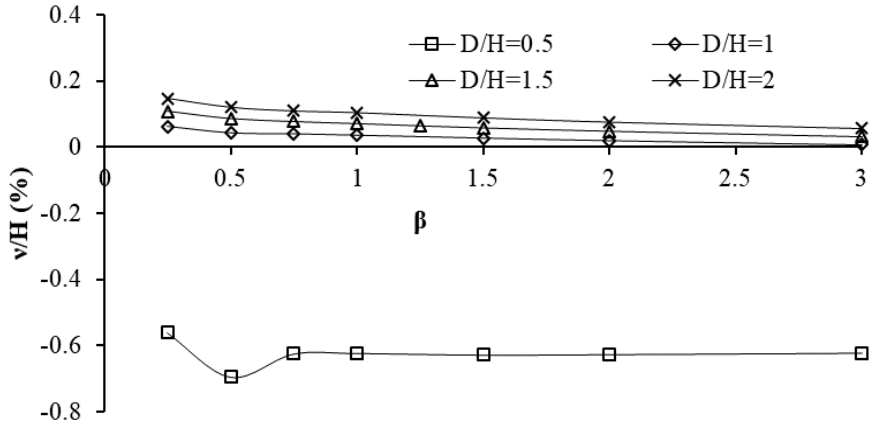

Fig. 23 Variation of normalized movement of ground surface with β for different embedded depths at λ=0.25 and Q=0.54 in dense sand

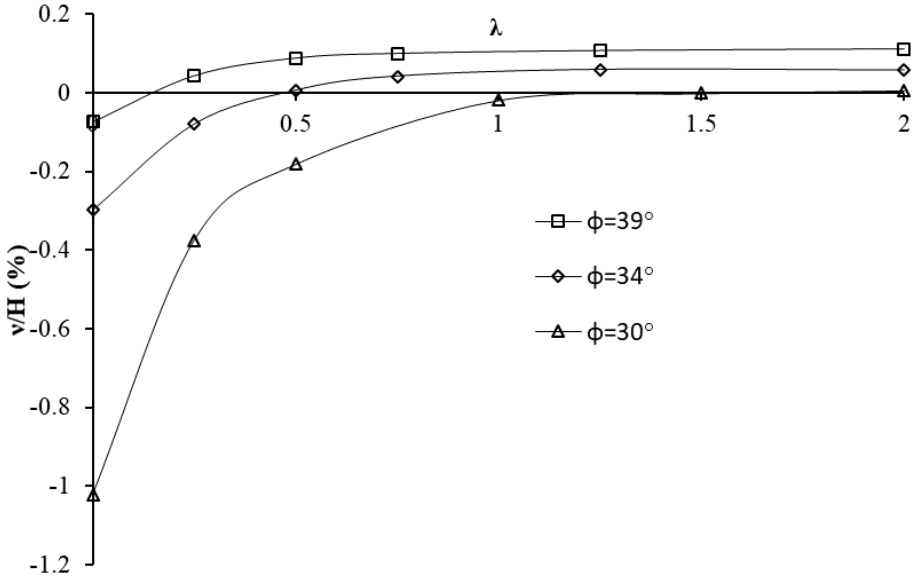

Fig. 24 Influence of different sand on movement of ground surface with λ at β=0.5, q=20 kPa and D/H=1

movement of the sheet pile wall which is regulated by the depth of embedment. The ground surface movement corresponding to different embedded depth are shown in Fig. 23 at the magnitude of surcharge load Q=0.54. As observed previously from Fig. 15 that for D/H=0.5, CSPW rotates about a greater depth than D/H=1, 1.5 and 2 which results in the more settlement of the ground surface adjacent to sheet pile wall. So, as observed from Fig. 23, more the embedded depth of the sheet pile wall, less settlement is observed. Furthermore, the denseness of sand increases the stiffness of soil which on the other hand increases the resisting capacity of the soil. So, the soil having more stiffness will have less settlement adjacent to the sheet pile wall as observed in Fig. 24. It shows that the normalized settlement adjacent to sheet pile wall observed are -0.0738%, -0.298% and -1.0225% for ϕ=39°, 34° and 30° respectively, i.e., more than 12 times settlement increase is observed in ϕ=30° from ϕ=39°.

5.5 Influence of distanced strip load on earth pressure

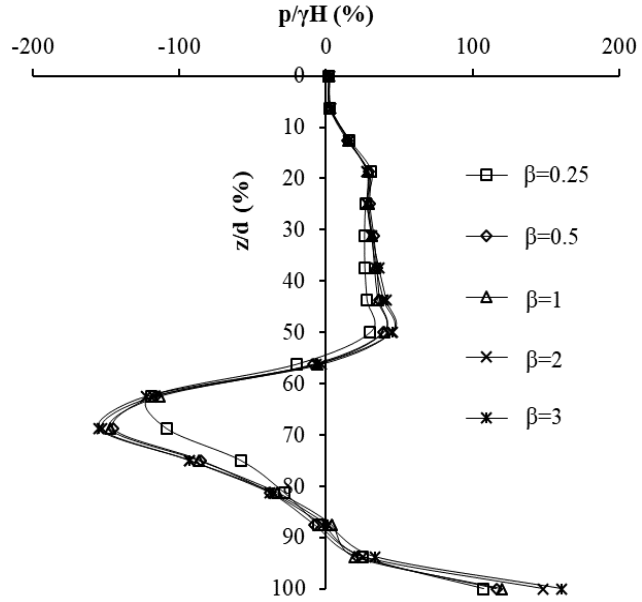

Fig. 25 Net earth pressure diagram of CSPW for different β at λ=0.25m and Q=2.72 with D/H=1 in dense sand

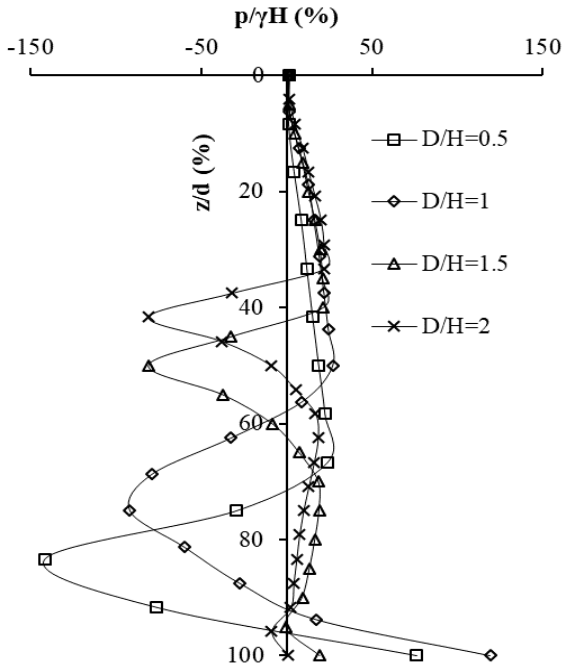

Fig. 26 Dependence of mobilization of earth pressure on embedded depth at λ=0.25, β=0.5 and Q=0.54 in dense sand

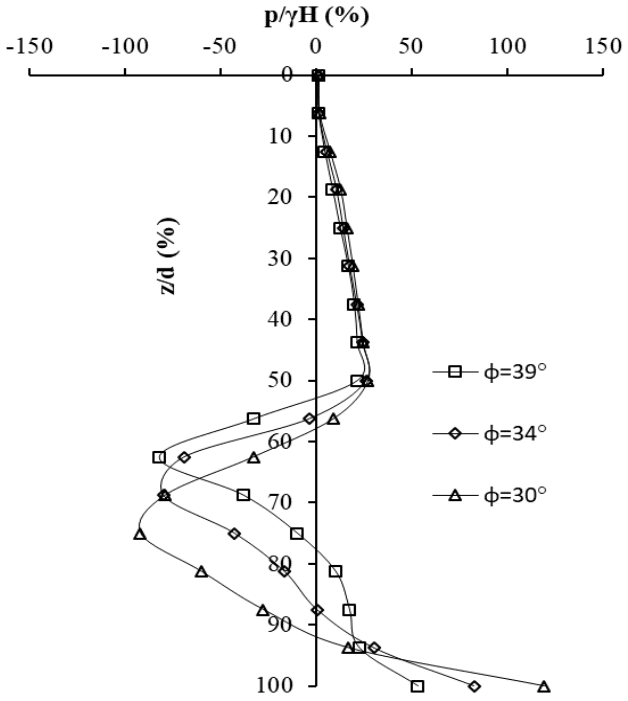

Fig. 27 Variation of normalized net earth pressure with normalized depth for different friction angles of sand at λ=0.25, β=0.5, q=20 kPa and D/H=1

Though the insertion of CSPW redistributes the stresses present in the soil, the placement of strip load at a distance adds in more redistribution of stresses depending on the depth of the embedment, friction angle and strip width ratio and results are represented in normalized horizontal earth pressure as ($p/\gamma H$) in percentage. Fig. 25 shows the net earth

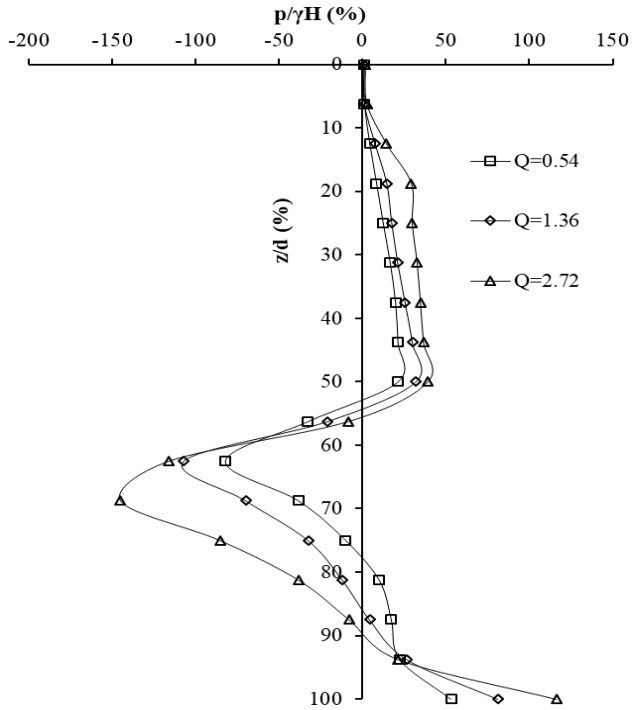

Fig. 28 Variation of normalized net earth pressure with normalized depth for different Q at λ=0.25, β=0.5 and D/H=1 in dense sand

pressure along with the depth of CSPW for different β at λ=0.25m and Q=2.72 in dense sand. It is observed that the maximum normalized net earth pressure increases with an increase in width of strip load. The increase in width of strip load increases the lateral earth pressure on the cantilever sheet pile wall which increases the net earth pressure along the length of the cantilever sheet pile wall. The mobilization of stresses can be clearly observed when the embedded depth of flexible CSPW increases as shown in Fig. 26. It shows that when D/H=0.5, the full mobilization of earth pressure in sheet pile wall takes place up to 83.33% of the length of the CSPW and as D/H increases to 1, 1.5 and 2, the depth of full mobilization reduces to 75%, 50% and 41.67% of the length of CSPW respectively. This is because as the embedded depth of the CSPW increases, the passive earth resistance decreases and it results to less mobilization of the earth pressure. The mobilization of stresses also depends on the stiffness of the present soil. As the sand with ϕ=39° has more resistance towards deformation, i.e., high stiffness, lateral stresses are less mobilized as compared to sand with ϕ=30° having less stiffness as observed in Fig. 27. The increase in the magnitude of strip load increases the lateral stresses on the sheet pile wall resulting in an increase in net earth pressure as shown in Fig. 28.

The influence of different height of exaction of CSPW on the lateral earth pressure along the depth for Q=0.54, λ=0.25 and β=0.5 are shown in Fig. 29. The depth of CSPW is taken constant as 12m and excavation heights are altered and the results for normalized earth pressure are shown in Fig. 29. It is observed from Fig. 29 that when the height of excavation of CSPW increases as D/H=5, 2, 1 and 0.5, the mobilization of earth pressure along the depth of

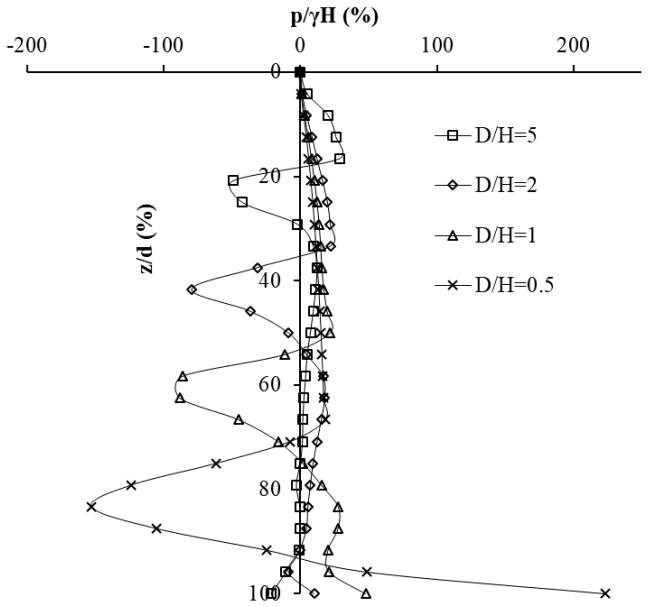

Fig. 29 Influence of different height if excavation on lateral earth pressure for Q=0.54, λ=0.25 and β=0.5 in dense sand

CSPW also increases. This is because when the height of excavation of the CSPW is less, the CSPW is stable and less passive earth resistance is required to provide stability and when the height of excavation of CSPW increases, the passive earth resistance below the dredge level increases to provide stability to the CSPW.

5.6 Influence of the depth of strip load below the ground level

Strip loads are not always placed on the ground surface. Strip loads in the form of buildings may be placed to a depth below the ground level (D_f). This type of surcharge applies pressure on the soil and should be considered for analysis. In the present study, a critical combination is used (λ=0.25 and β=0.5) to analyze the influence of strip load placed at a depth below ground level on flexible CSPW.

Figs. 30-32 highlight the trend of normalized maximum bending moment, deflection and movement of the ground surface with respect to the strip load present below the ground level for the magnitude Q=0.54, 1.36 and 2.72. From Fig. 30, it is clearly observed that there is a significant decrease (59%) in the magnitude of normalized bending moment when the strip load is moved deeper from ground surface to D_f/H=0.5 for Q=2.72 while for Q=1.36 and 0.54, the reduction in the normalized bending moment are 40% and 24.5% respectively. Further increment of the depth of strip load below the ground level decreases the normalized bending moment and the influence of the magnitude of strip load vanishes beyond D_f/H=0.75. A similar trend is also observed for deflection as shown in Fig. 31. The deflection at the top of the wall reduces by 72.4%, 68% and 17% for Q=2.72, 1.36 and 0.54 when the strip load is moved deeper to D_f/H=0.125 from ground surface (D_f/H=0). This is attributed to an increase in vertical stress below foundation level at a deeper depth and hence increase in the lateral earth pressure is moved downward and thus the reduction in rotation decreases the deflection. The movement of the ground surface adjacent to the sheet pile experiences the settlement for Q=2.72, heaving for Q=0.54 and both settlement at D_f/H=0 as well as heaving at D_f/H>0.125 for Q=1.36 as shown in Fig. 32. The rate of movement of the ground surface decreases as the depth of strip load below the ground level increases and the rate vanishes near D_f/H=0.75.

6. Conclusions and recommendation

6.1 Conclusions

In the present study, the CSPW are analyzed using the

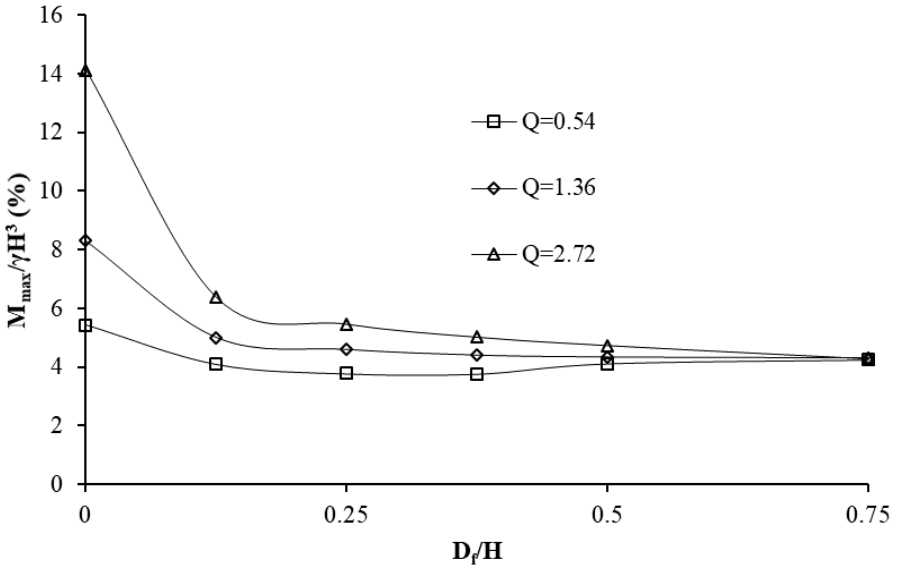

Fig. 30 Variation of normalized bending moment with D_f/H for different magnitudes of strip load at λ=0.25, β=0.5, D/H=1 in dense sand

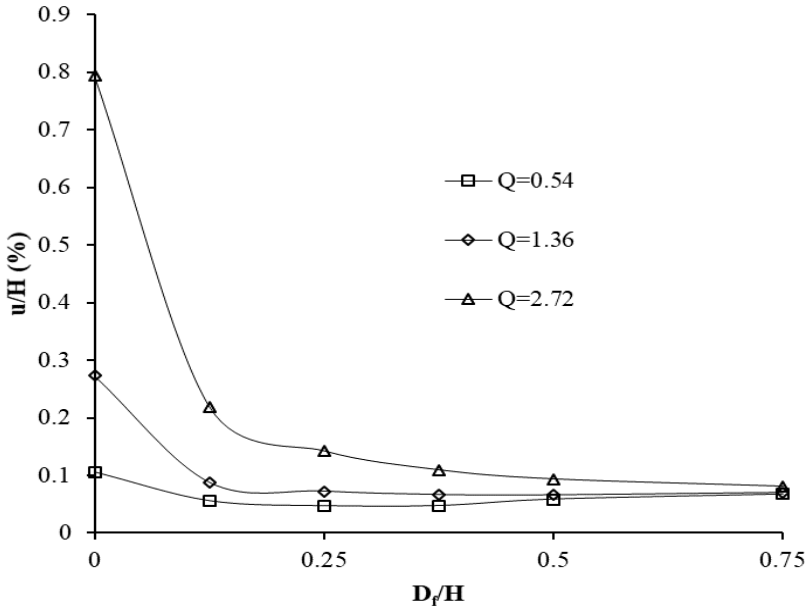

Fig. 31 Variation of normalized deflection with D_f/H for different strip load at λ=0.25, β=0.5, D/H=1 in dense sand

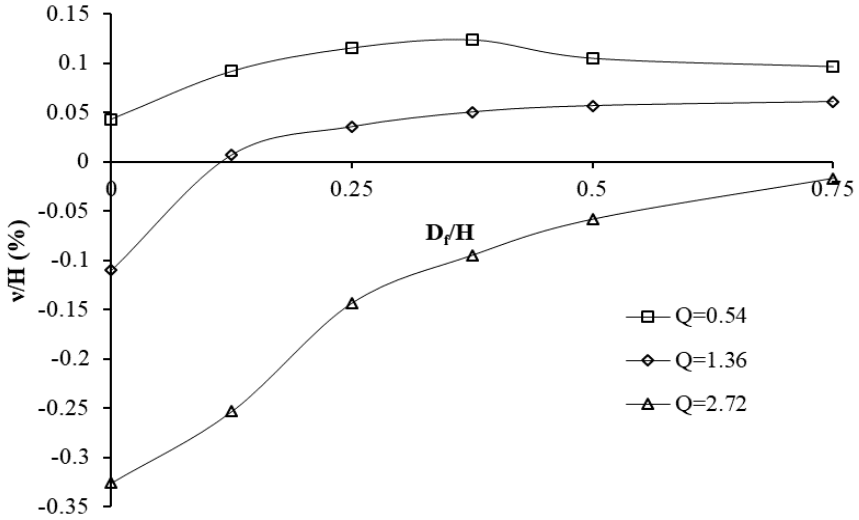

Fig. 32 Influence of magnitude of strip load on movement of ground surface with D_f/H at λ=0.25, β=0.5, D/H=1 in dense sand

finite-difference based computer program FLAC2D for different locations of strip load on backfill and its width in three different soil conditions. The numerical model with strip loading is validated with the existing bending moment results of Georgiadis and Anagnostopoulos (1998). The following major conclusions are drawn from the present study:

- The bending moment, earth pressure, deflection of CSPW and settlement of ground surface are maximum when the strip load is situated at the top of the wall (λ=0) with strip width ratio (β)=0.5. The effect of strip load can be totally neglected beyond λ=2. However, for practical case, the optimum combination to analyze CSPW is λ=0.25 and β=0.5.
- At low embedded depth (about 33% of total length), CSPW is on the verge of instability and becomes stable as embedded depth increases.
- The mobilization of earth pressure is at greater depth in sheet pile wall having low embedded depth with high magnitude of surcharge in loose sand.
- The behavior of sheet pile walls changes for embedded depths with respect to the location of strip load. When strip load is placed on the wall, the behavior for D/H=0.5 is different than others and at $\lambda \geq 0.5$, the CSPW having $D \geq H$ and $D \leq H$ show similar results.
- The height of excavation influences the behavior of CSPW. Lesser the height of excavation, more stable is the cantilever sheet pile wall.
- The influence of strip load is maximum when placed on the ground surface and decreases as the strip load is placed at a depth below the ground surface for the same magnitude of stress. The influence of depth of strip load below ground level vanishes beyond D_f =0.75 H.

Thus, if the cantilever sheet pile wall is designed to

ensure the safety of excavation, then a suitable embedded depth must be chosen, as much increase in the depth of excavation is not an economical option.

6.2 Limitations and recommendations

Although this paper has addressed the different factors affecting the performance of cantilever sheet pile wall due to placement of strip load, there are still some limitations. These limitations are presented here with recommendations for future research.

- In this study, the soil is modeled using elastic-plastic Mohr-Coulomb model. In future research, other constitutive models can also be used.
- A detailed field testing is required to support the findings presented here.
- This study has mainly focused on the static condition. Future research should investigate under dynamic loading conditions.
- The influence of cohesive soil on cantilever sheet pile wall can also be seen in future research.
- Two types of soil may be considered.
- In place of cantilever sheet pile wall, anchored sheet pile wall can be placed.
- The effect of water table can also be considered in the future research.

References

Ahmad, H., Hoseini, M.H., Mahboubi, A., Noorzad, A. and Zamanian, M. (2021), "Effect of sheet pile wall on the load-settlement behaviour of square footing nearby excavation", *Geomech. Geoeng.*, 1-19. https://doi.org/10.1080/17486025.2021.2019320.

Ahmadi, A. and Ahmadi, M.M. (2019), "Three-dimensional numerical analysis of corner effect of an excavation supported by ground anchors", *Int. J. Geotech. Eng.*, 1-13. https://doi.org/10.1080/19386362.2019.1682349.

Beygi, M., Vali, R., Porhoseini, R., Keshavarz, A. and Maleksaeedi, E. (2021), "The effect of rotational stiffness on the behaviour of retaining wall", *Int. J. Geotech. Eng.*, **15**(7), 845-856. https://doi.org/10.1080/19386362.2018.1517927.

Bilgin, O. (2010), "Numerical studies of anchored sheet pile wall behavior constructed in cut and fill conditions", *Comput. Geotech.*, **37**, 399-407. https://doi.org/10.1016/j.compgeo.2010.01.002.

Blum, H. (1931), *Einspannungs Verhaeltnisse Bei Bohlwerken*, W. Ernst and Sohn, Berlin.

Bowles, J.E. (2012), *Foundation Analysis and Design*, 5th Edition, McGraw Hill, New York.

Callisto, L. (2014), "Capacity design of embedded retaining structures", *Géotechnique*, **64**(3), 204-214. https://doi.org/10.1680/geot.13.P.091.

Callisto, L. and Soccodato, F.M. (2010), "Seismic design of flexible cantilevered retaining walls", *J. Geotech. Geoenviron. Eng.*, **136**(2), 344-354. https://doi.org/10.1061/(ASCE)GT.1943-5606.0000216.

Caltabiano, S., Cascone, E. and Maugeri, M. (2012), "Static and seismic limit equilibrium analysis of sliding retaining walls under different surcharge conditions", *Soil Dyn. Earthq. Eng.*, **37**, 38-55. https://doi.org/10.1016/j.soildyn.2012.01.015.

Chowdhury, S.S., Deb, K. and Sengupta, A. (2016), "Effect of fines on behavior of braced excavation in sand: Experimental and numerical study", *Int. J. Geomech.*, **16**(1), 04015018-1-04015018-13. https://doi.org/10.1061/(ASCE)GM.1943-5622.0000487.

Conte, E., Troncone, A. and Vena, M. (2017), "A method for the design of embedded cantilever retaining walls under static and seismic loading", *Géotechnique*, **67**(12), 1081-1089. https://doi.org/10.1680/jgeot.16.P.201.

Conti, R., Viggiani, G.M.B. and Buralid'Arezzo, F. (2014), "Some remarks on the seismic behaviour of embedded cantilevered retaining walls", *Géotechnique*, **64**(1), 40-50. https://doi.org/10.1680/geot.13.P.031.

Conti. R. and Viggiani. G.M.B. (2013), "A new limit equilibrium method for the pseudostatic design of embedded cantilevered retaining walls", *Soil Dyn. Earthq. Eng.*, **50**, 143-150. https://doi.org/10.1016/j.soildyn.2013.03.008..

Day, R.A. (1999), "Net pressure analysis of cantilever sheet pile walls", *Géotechnique*, **49**(2), 231-245. https://doi.org/10.1680/geot.1999.49.2.231.

Doubrovskya, M.P. and Meshcheryakov, G.N. (2015), "Physical modeling of sheet piles behavior to improve their numerical modeling and design", *Soil. Found.*, **55**(4), 691-702. https://doi.org/10.1016/j.sandf.2015.06.003.

El-Emam, M. and Touqan, M. (2020), "Experimental modeling of strip footing adjacent to non-yielding retaining wall", *Innov. Infrastr. Solution.*, **5**(2), 1-17. https://doi.org/10.1007/s41062-020-00288-w.

El Sawwaf, M. (2010), "Experimental and numerical study of strip footing supported on stabilized sand slope", *Geotech. Geolog. Eng.*, **28**, 311-323. https://doi.org/10.1007/s10706-009-9293-9.

Gaba, A., Hardy, S., Doughty, L., Powrie, W. and Selemetas, D. (2017), *Guidance on Embedded Retaining Wall Design*, CIRIA C760, London, UK.

Gazan, S. (2011), "Normalized relationships for depth of embedment of sheet pile walls and soldier pile walls in cohesionless soils", *Soil. Found.*, **51**(3), 559-564. https://doi.org/10.3208/sandf.51.559.

Georgiadis, M. and Anagnostopoulos, C. (1998), "Lateral pressure on sheet pile walls due to strip load", *J. Geotech. Geoenviron. Eng.*, **124**(1), 95-98. https://doi.org/10.1061/(ASCE)1090-0241(1998)124:1(95).

Ghadrdan, M., Shaghaghi, T. and Tolooiyan, A. (2020), "Sensitivity of the stability assessment of a deep excavation to the material characterisations and analysis methods", *Geomech. Geophys. Geo-Energy Geo-Resour.*, **6**(59), 1-14. https://doi.org/10.1007/s40948-020-00186-6.

Hazzar, L., Hussien, M.N. and Karray, M. (2020), "Two-dimensional modelling evaluation of laterally loaded piles based on three-dimensional analyses", *Geomech. Geoeng.*, **15**(4), 263-280. https://doi.org/10.1080/17486025.2019.1640897.

Hsiung, B.C.B., Likitlersuang, S., Phan, K.H. and Pisitsopon, P. (2021), "Impacts of the plane strain ratio on excavations in soft alluvium deposits", *Acta Geotechnica*, **16**, 1923-1938. https://doi.org/10.1007/s11440-020-01115-3.

Itasca (2016), User's Guide for FLAC2D, Version 8.0, Itasca Consulting Group, Minneapolis, Minnesota, U.S.A.

Jao, M., Ahmed, F., Sudani, G., Nguyen, T.T.M. and Wang, M.C. (2017), "Interaction between strip footings and sheet pile walls", *Elec. J. Geotech. Eng.*, **22**(6), 1655-1674.

Jiang, S., Du, C. and Sun, L. (2018), "Numerical analysis of sheet pile wall structure considering soil-structure interaction", *Geomech. Eng.*, **16**(3), 309-320. https://doi.org/10.12989/gae.2018.16.3.309.

King, G.J.W. (1995), "Analysis of cantilever sheet-pile walls in cohesionless soil", *J. Geotech. Eng.*, **121**(9), 629-635. https://doi.org/10.1061/(ASCE)0733-9410(1995)121:9(629).

Krabbenhoft, K. (2019), "Plastic design of embedded retaining walls", *Proc. Inst. Civil Eng.-Geotech. Eng.*, **172**(2), 131-144.

https://doi.org/10.1680/jgeen.17.00151.
Krey, H. (1936), *Erddruck*, 5th Edition, Erdwiderstand, Berlin.
Nguyen, T.S. and Likitlersuang, S. (2021), "Influence of the spatial variability of soil shear strength on deep excavation: A case study of a bangkok underground MRT station", *Int. J. Geomech.*, **21**(2), 04020248-1-12. https://doi.org/10.1061/(ASCE)GM.1943-5622.0001914.
Nucor Skyline (2017), Technical Product Manual, New Jersey, USA. https://www.nucorskyline.com.
Padfield, C.J. and Mair, R.J. (1984), "Design of retaining walls embedded in stiff clays", Report 104, Construction Industry Research and Information Association (CIRIA), London, UK.
Qu, H., Li, R., Hu, H., Jia, H. and Zhang, J. (2016), "An approach of seismic design for sheet pile retaining wall based on capacity spectrum method", *Geomech. Eng.*, **11**(2), 309-323. https://doi.org/10.12989/gae.2016.11.2.309.
Samadhiya, N.K. (2019), "Evaluation of model sheet pile wall adjacent to a strip footing-An experimental investigation", *Int. J. Geotech. Eng.*, **14**(7), 828-835. https://doi.org/10.1080/19386362.2019.1581459.
Singh, A.P. and Chatterjee, K. (2020a), "A simplified method for seismic design of cantilever sheet pile walls under infinite uniform surcharge load", *Int. J. Geomech.*, **20**(9), 04020139-1_04020139-11. https://doi.org/10.1061/(ASCE)GM.1943-5622.0001764.
Singh, A.P. and Chatterjee, K. (2020b), "Ground settlement and deflection response of cantilever sheet pile wall subjected to surcharge loading", *Ind. Geotech. J.*, **50**(4), 540-549. https://doi.org/10.1007/s40098-019-00387-1.
Singh, A.P. and Chatterjee, K. (2020c), "Influence of soil type on static response of cantilever sheet pile walls under surcharge loading: a numerical study", *Arab. J. Geosci.*, **13**(3), 138-1-11. https://doi.org/10.1007/s12517-020-5170-x.
Singh, A.P. and Chatterjee, K. (2020d), "Lateral earth pressure and bending moment on sheet pile walls due to uniform surcharge", *Geomech. Eng.*, **23**(1), 71-83. https://doi.org/10.12989/gae.2020.23.1.071.
Singh, A.P. and Chatterjee, K. (2021a), "A displacement based approach for seismic analysis and design of cantilever sheet pile walls under surcharge loading", *Comput. Geotech.*, **140**, 104481-1-11. https://doi.org/10.1016/j.compgeo.2021.104481.
Singh, A.P. and Chatterjee, K. (2021b), "Effect of soil-wall friction angle on behaviour of sheet pile wall under surcharge loading", *Proc. Nat. Acad. Sci., India Section A: Phys. Sci.*, **91**(1), 169-179. https://doi.org/10.1007/s40010-020-00657-1.
Singh, A.P. and Chatterjee, K. (2022a), "Seismic analysis of cantilever sheet pile walls with strip load for any lateral deformation", *Int. J. Geomech.*, **22**(5), 04022039-1-11. https://doi.org/10.1061/(ASCE)GM.1943-5622.0002352.
Singh, A.P. and Chatterjee, K. (2022b), "The influence of strip load on the seismic design of cantilever sheet pile walls: A simplified analytical solution", *Bull. Earthq. Eng.*, 1-22. https://doi.org/10.1007/s10518-022-01409-9.
Steenfelt, J.S. and Hansen, B. (1984), "Sheet pile design earth pressure for strip load", *J. Geotech. Eng.*, **110**(7), 976-986. https://doi.org/10.1061/(ASCE)0733-9410(1984)110:7(976).
Sudani, G.A., Brake, N. and Jao, M. (2015), "Stability of footings adjacent to pile walls", *Int. J. Geomech.*, **15**(6), 04015006-1-11. https://doi.org/10.1061/(ASCE)GM.1943-5622.0000480.
Terzaghi, K. (1954), "Anchored bulkheads", *Trans.*, **119**, 1243-1324. https://doi.org/10.1061/TACEAT.0007100.
Wolf, J.P. and Song, C. (2002), "Some cornerstones of dynamic soil-structure interaction", *Eng. Struct.*, **24**(1), 13-28. https://doi.org/10.1016/S0141-0296(01)00082-7.

List of symbols

D	embedded depth
d	total length of cantilever sheet pile walls
D_f	depth of strip load
E	modulus of elasticity
EI	flexural rigidity
G	shear modulus
H	height of excavation
I	moment of inertia
K	bulk modulus
K_n	normal stiffness
K_s	shear stiffness
M	bending moment
p	horizontal earth pressure
q	magnitude of strip load
Q	normalized magnitude of strip load
u	deflection of cantilever sheet pile walls
x	distance from cantilever sheet pile walls
z	depth measured below ground level
β	normalized width of strip load
γ	unit weight of soil
δ	soil-wall interface friction angle
$\Delta z_{\min}$	smallest width of adjoining zone in normal direction to the interface
λ	normalized distance of the strip load from the top of the wall
μ	Poisson's ratio
v	movement of the ground surface
ϕ	soil friction angle